Semi-Annual Progress Report

ANALYTICAL TECHNIQUES FOR IDENTIFICATION AND STUDY OF ORGANIC MATTER IN RETURNED LUNAR SAMPLES

Supported by

NASA Contract
NAS 9-7889

FEB 17 1971

Manned Spacecraft Center
Houston, Texas 77058

Space Sciences Laboratory Series 10, Issue 35

UNIVERSITY OF CALIFORNIA, BERKELEY

CR-114164

Space Sciences Laboratory
University of California
Berkeley, California 94720

Semi-Annual Report

on

ANALYTICAL TECHNIQUES FOR IDENTIFICATION AND STUDY OF ORGANIC MATTER IN RETURNED LUNAR SAMPLES

Supported by
NASA Contract NAS 9-7889

For the Period
October 1, 1968 — March 31, 1969

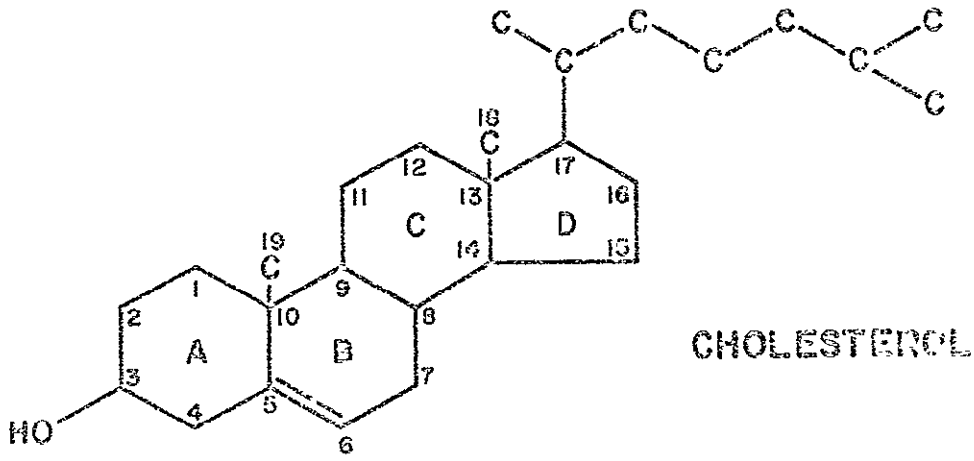

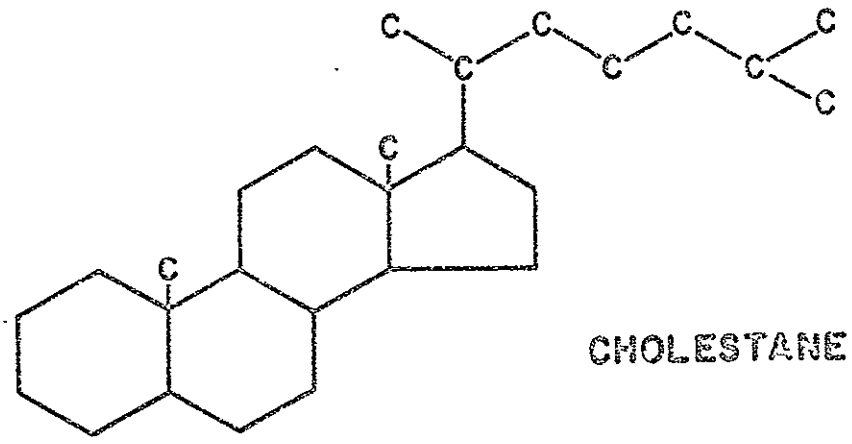

FIGURE 5.

Structures of a Steriod and its Corresponding Sterane.

ANALYTICAL TECHNIQUES FOR IDENTIFICATION AND STUDY OF ORGANIC MATTER IN RETURNED LUNAR SAMPLES

NASA Contract NAS 9-7889
October 1, 1968 – March 31, 1969

Introduction

A broad base of experience in organic geochemistry and organic mass spectrometry is laying the foundation for the analysis of organic material in the returned lunar samples. The emphasis in on the utilization and development of computerized mass spectrometry as a most sensitive and versatile tool for the identification of organic material.

Making up the first part of this report are studies in organic geochemistry which deal with the isolation and identification of individual organic compounds from various types of terrestrial and extra-terrestrial samples. The diversity of the samples and compound classes studied has added substantially to our knowledge in this area. A particularly fortuitous occurrence was the fall of a meteorite near Pueblito de Allende, Chihuahua, Mexico. Our experience with this extra-terrestrial sample will provide a model sample in preparing for the analysis of the returned lunar samples.

Closely associated with the geochemistry program are investigations into the fundamental nature of fragmentation processes occurring in the ion source in the mass spectrometer. The second part of the report consists of these organic mass spectrometry investigations, including both electron impact and field ionization phenomena.

The next two sections of this report are intimately associated with the Apollo program. The development of a computer-coupled low resolution mass spectrometer system for the Lunar Receiving Laboratory is described. This system will perform in the preliminary analysis of the returned lunar sample. A detailed report on the exhaust gas sampling from the lunar module descent engine follows.

During this period our facilities were expanded to include two new mass spectrometers whose essential analytical functions are described in the last section of this report. The planned cleanroom facility, necessary for lunar sample analysis, is also discussed.

I. ORGANIC GEOCHEMISTRY

Organic Analysis on the Pueblito de Allende Meteorite

On February 8, 1969, a meteorite fell near Pueblito de Allende, Chihuahua, Mexico. An elemental analysis of fragments of it, collected shortly thereafter, was published [E. King *et al.*, *Science 163*, 928 (1969)] and showed that it contained carbon to an extent of approximately 0.3%. In the meantime, samples of the meteorite were collected by one of us (B.R.S.). The largest meteorite fragment obtained was 13.381 kg (cf. *Figure 1*) with smaller specimen of 2.475 kg, 1.706 kg, and 0.453 kg. The smaller fragment (*Figure 2*) weighing 2.475 kg and having a fusion crust over its entire surface was used for the organic analysis. We report here the preliminary analysis for certain organic constituents in that sample, which was collected on February 15, 1969.

The surface of a 240 gram portion upon which the analysis was to be performed was first removed to a depth of about 1/4 inch, including all of the fusion crust as well as an approximately equivalent thickness of the fresh break which represented one surface. This operation, and all succeeding operations, were carried out in a clean cabinet through which a filtered air stream was passing continously. The chips and center piece were analyzed separately.

The extractable organic compounds are shown in the chromatogram in *Figures 3* and *4*; in each case the *A* chromatogram represents the analysis of the surface chips and the *B* chromatogram represents the analysis of the interior of the sample. The surface chips contained 0.1 and 0.5 ppm, as indicated specifically in the figures, while the interiors contained 0.001 ppm as indicated. The identity of each peak was obtained by combined gas chromatography-mass spectrometry (Aerograph 204 — GEC AEI MS. 12 and PE 900 — PE 270). The chromatogram of the organic extract obtained from HF-HCl dissolution revealed no organic material whatsoever,

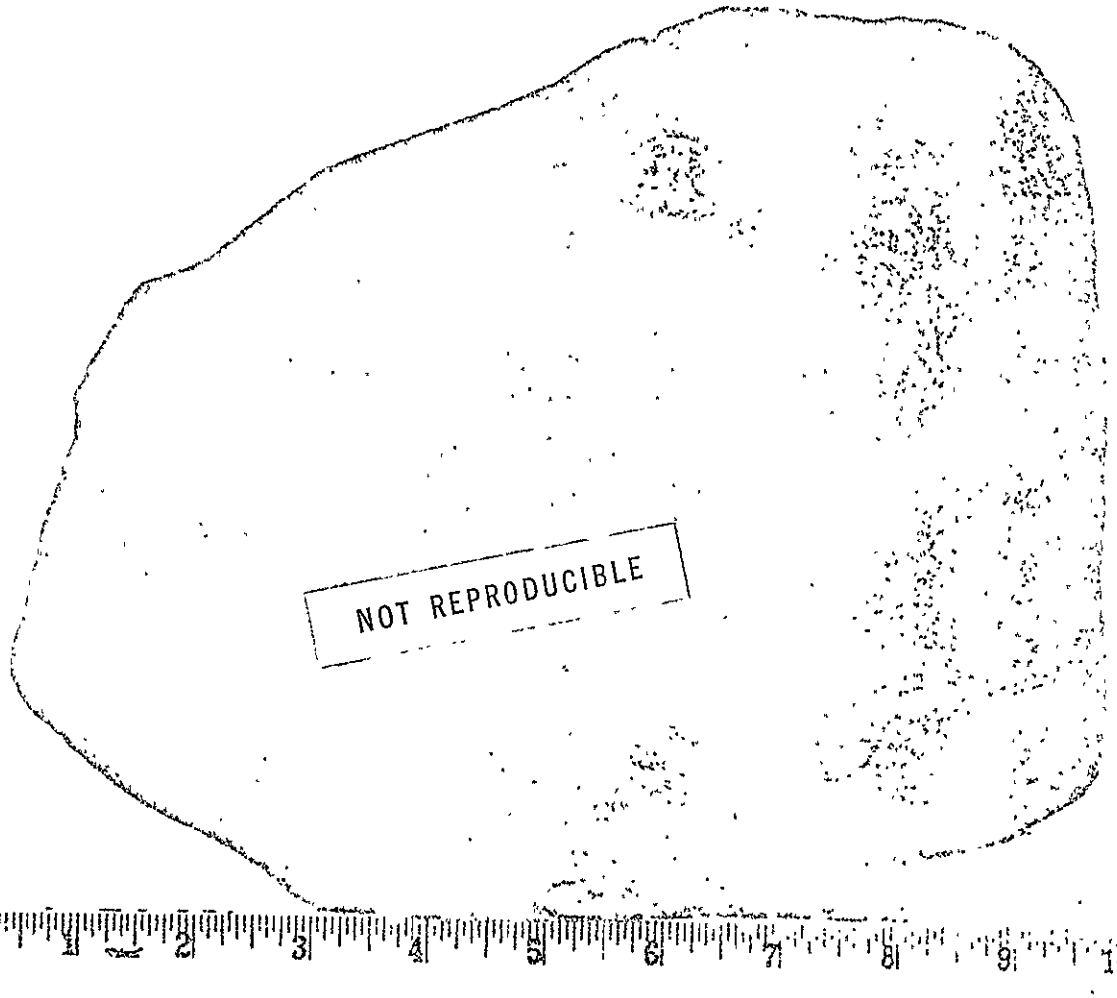
NOT REPRODUCIBLE

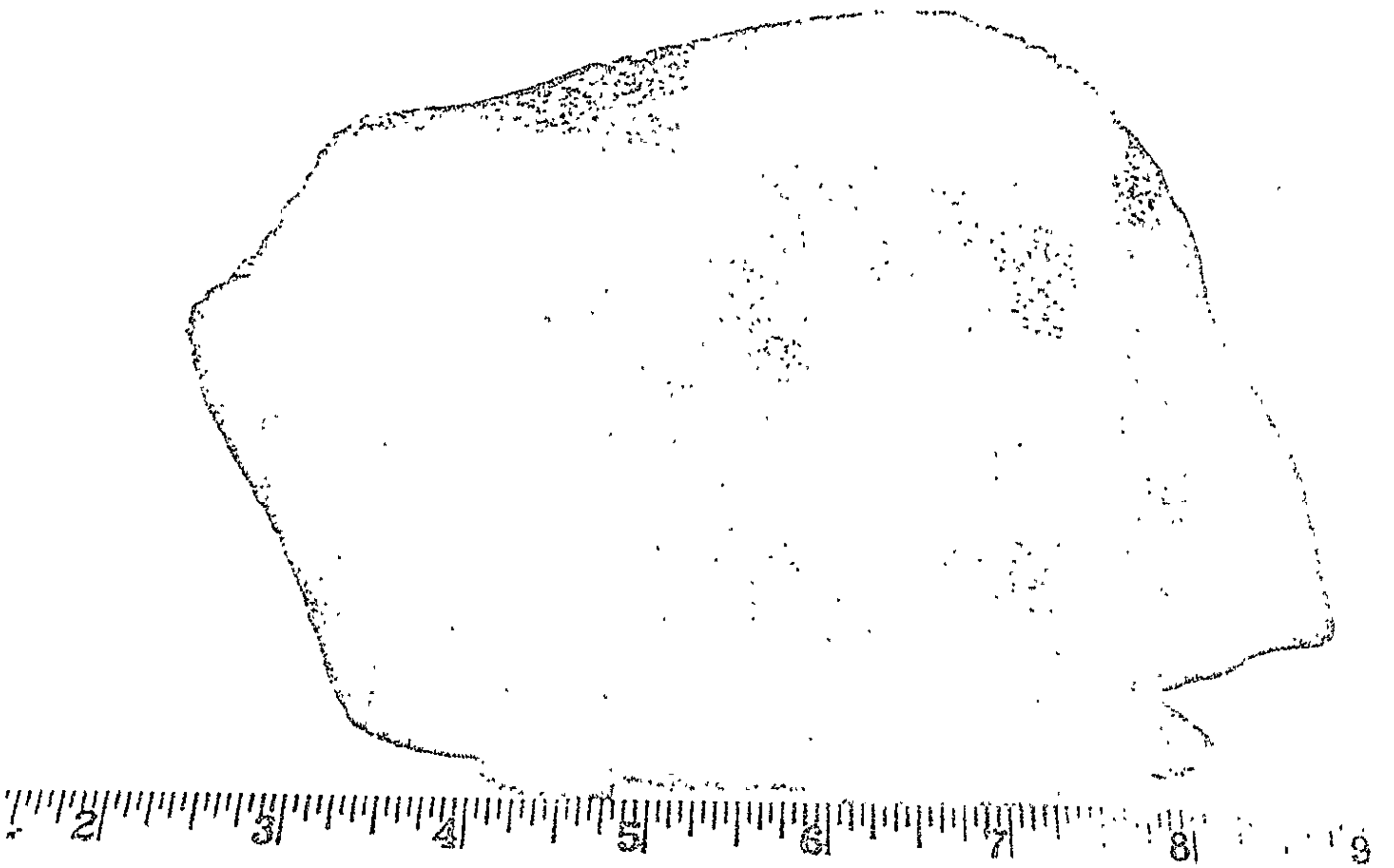

FIGURE 2. The fragment of the Pueblito de Allende meteorite (2.4[illegible] kg) used for [illegible]

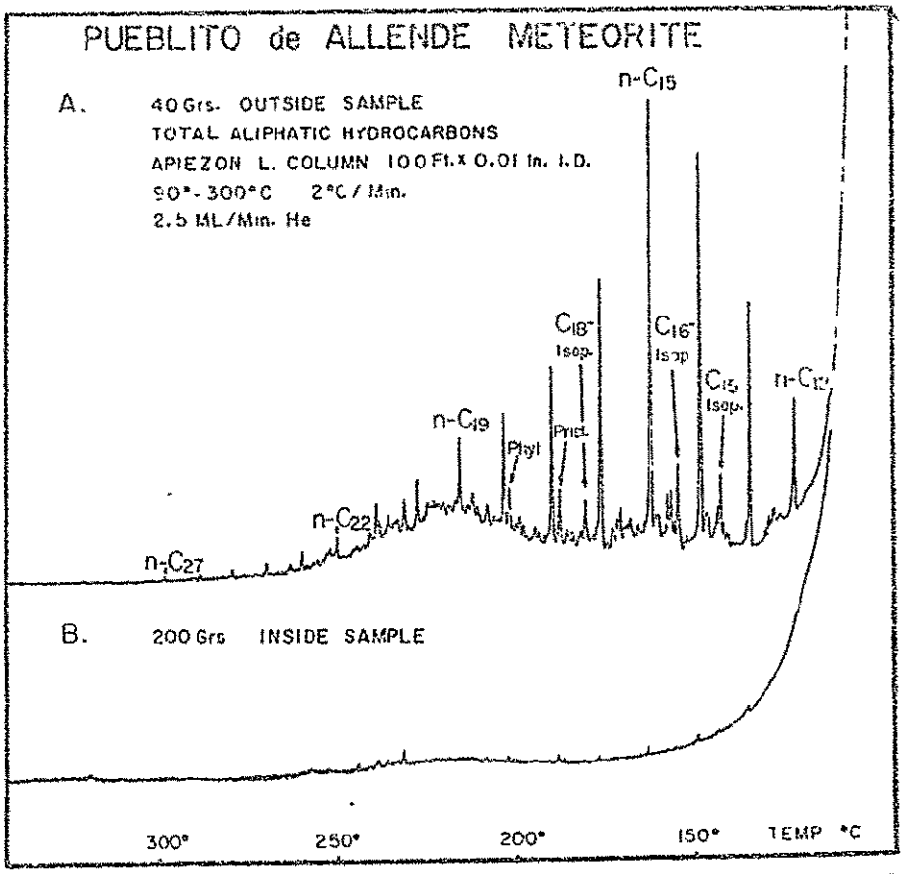

FIGURE 3

Gas chromatogram of total aliphatic hydrocarbons from extractable organic material. Aerograph Model 204 gas chromatograph equipped with a flame ionization detector. About 1/10 of the n-heptane eluate was injected in each case.

A. 0.5 ppm of hydrocarbons were detected in outside sample.

B. 0.001 ppm of hydrocarbons were detected in interior sample.

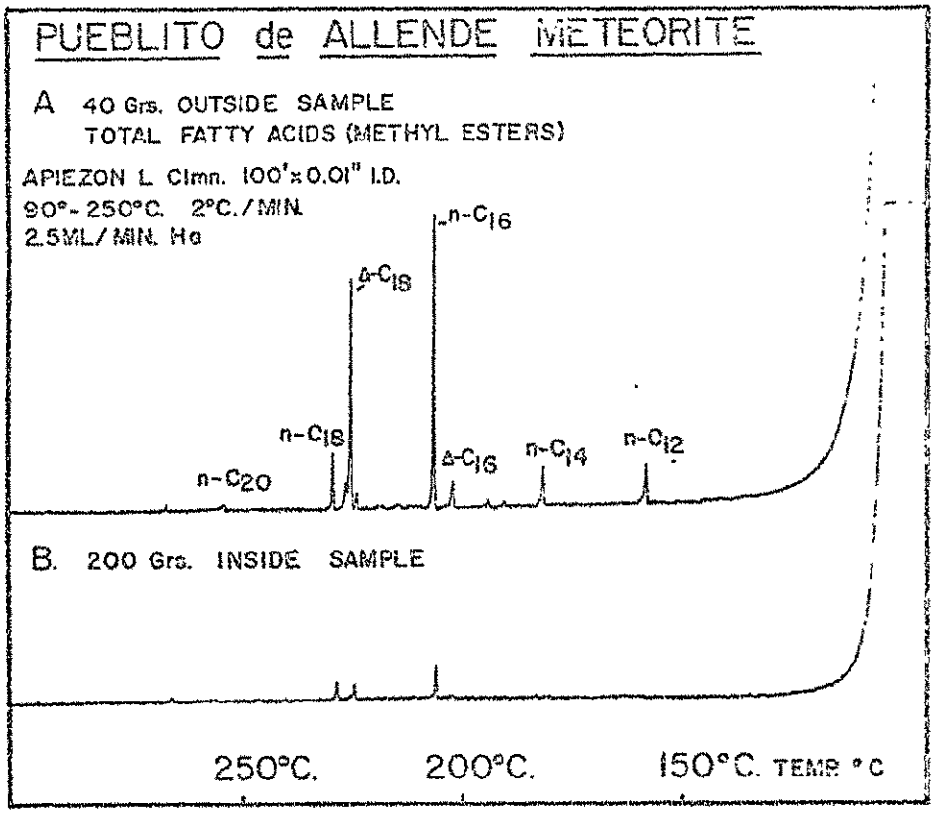

Fig. 4. Gaschromatogram of total fatty acids (methyl esters) from extracted organic matter.
A. 3.1 ppm of fatty acids were found in outside sample.
B. 3.3µl ppm of fatty acids were found in interior sample.

which indicates the polar organics are bound to, or trapped in the mineral matrix as metal salts.

It is quite clear that the organic material found in the surface layer of this meteorite is of biological origin and can hardly be other than terrestrial contamination acquired even in the short period of time available to the meteorite, namely, between its fall on February 8, 1969, and its collection on February 15, 1969. The speed with which this contamination was acquired and the diversity of the material contained in that contamination make doubtful any interpretation of such organic materials as have been found in meteorites of unknown, or at least considerably longer, terrestrial history. The presence of the mono-unsaturated C_{18} fatty acid (cf. Fig. 4) in the Pueblito de Allende meteorite is additional confirmation of recent contamination. Furthermore this exercise in analysis of rock recently acquired on earth makes all the more clear the need for the extreme precautions that are being taken in preserving the integrity of the returned lunar sample.

Work is continuing on the organics derived by chromic acid oxidation of the carbonaceous concentrate from the demineralization. A soil sample from an impact crater is also being examined for its contribution to the organic contamination. A more detailed examination under clean room conditions is planned on a larger sample where it is then possible to examine the organic matter at various depths within the sample. Various pyrolysis experiments, both here at Berkeley and at the LRL in Houston, are in progress.

Optically Active Steranes in a Miocene Crude Oil

Optical activity is the ability of a homogeneous solution of a chemical compound to rotate the plane of polarized light. It is due to centers of asymmetry in molecules. It is possible under very special and rare conditions to generate asymmetric molecules by purely physical means. However, living organisms perform this synthesis routinely. Thus, the existence of optically active substances in a material is evidence of the intervention of the chemical process of cells. This evidence is strengthened when, as will be shown, the molecules responsible for the activity have close structural relationship to known cell biochemicals.

The optical activity of many petroleums is due to the presence of ring saturated hydrocarbons. The molecules responsible are believed to have the sterane and triterpane structures, although relatively few specific compounds have been reported in the literature. Molecules of this type are of great importance as fossil biochemicals in the study of biochemistry of ancient terrestrial sedimentary rocks and of great importance in returned lunar material. The optically active fractions of petroleum are extremely complex mixtures and the separation of pure species from them is a major problem. In order to limit the magnitude of the problem, attention has been focused on methods of isolating steranes hydrocarbons. The obvious structural relationship between a common steroid, cholesterol, and a sterane hydrocarbon is shown in Figure 1. The two types of steranes considered in this work correspond to the 5 α and 5 β steroids encountered in living organisms. These isomers differ only in the stereochemistry of the juncture of rings A and B. There is a vast chemical and biological literature on the steroids, but a much smaller one on the steranes.

This report describes progress on the development of a procedure for isolating sterane hydrocarbons in samples of organic geochemical interest. A crude oil was selected for the initial development in order to have relatively large amounts of material available. Dr. George Phillippi of the Shell Development Company, Houston, Texas, kindly provided a large sample of a Miocene crude oil from a producing well in the Los Angeles Basin, California. It had been shown by mass spectrometric type analysis that this crude oil was rich in four-ring saturated hydrocarbons and would be highly suitable for initial work.

The work has been greatly facilitated by recent advances in the measurement of optical activity. The Bendix-Ericson Automatic Polarimeter is capable of routinely detecting 0.001 degrees of optical rotation. With special care, it is possible to detect 0.0003 degrees. This makes possible the measurement of samples that are one to two orders of magnitude smaller than those used in conventional polarimetry.

An outline of the procedure that has evolved is as follows: The isolation of an aromatic free, saturated hydrocarbon fraction by urea precipitation, silica gel column chromatography, treatment with cold, fuming sulfuric acid, and alumina column chromatography. Other aspects of

normal alkanes by urea adductination. *(c)* A simple distillation of the samples into two fractions, a low boiling one from C_{14} to C_{24} and a high boiling fraction with carbon number greater than 24. *(d)* The thiourea adductination of the low boiling C_{14} to C_{24} fraction in order to concentrate the isoprenoid hydrocarbons, which are the major hydrocarbon constituents of the oil. *(e)* The fractionation of the low boiling thiourea adduct into twenty-four narrow boiling fractions. A semi-micro vacuum spinning band distillation column was used. *(f)* The fractionation of the high boiling hydrocarbons into fourteen narrow boiling range fractions. Six of these fractions contain over eighty five percent of the optical activity in the crude oil. *(g)* The thiourea adductionation of the six high boiling fractions containing the highes concentration of optical activity. *(h)* The initial concentration of four ring hydrocarbons by chromatography with a 12 foot by 1/2 inch column of Sephadex LH-20 using acetone-tetrahydrofuran, 1/1, as expander and eluant. *(i)* Further fractionation of the concentrates from (h) on a 25 foot by 3/8 inch column of alumina using hexane as eluant. *(j)* The isolation of major components in fractions from (step i) by preparative gas-liquid chromatography using 1/8 inch diameter packed columns. *(k)* The identification of single "peaks" from (j) by capillary-column gas chromatography and by mass spectrometry.

An indication of the complexity of the mixture is given by the fact that this lengthy separation procedure has yielded small amounts of optically active steranes of 60 to 80 percent purity.

Several points, which have shown up during the development of the procedure, are of interest. No optical activity has been detected in the fractions isolated in (step e). Gas chromatography has shown that three of them are greater than seventy percent phytane and three of them are rich in pristane. The specific rotations of these fractions are less than 0.03 degrees per decimeter per gram per milliter. This contrasted to specific rotations of 4 or greater in the high boiling fractions of (step f). If the phytyl side chain of chlorophyll is the source material for the isoprenoid hydrocarbons phytane and pristane, one would expect them to be optically active. A different source material and route to phytane and pristane is indicated.

The experience in (step g), the thiourea adductination of steranes, is similar to that of Eglinton, who worked in this laboratory several years ago. Certain steranes unexpectedly form stable thiourea adducts. One would predict that they are too large to fit in the channels of the thiourea crystals. Studies in this area are hampered by the lack of synthetic, pure, ring hydrocarbons. Careful analysis of the adduct and non-adduct fractions in this work may give valuable information on the structures of adduct forming molecules.

The fractionation of hydrocarbon types by long alumina columns have worked surprisingly well (step i). The separations possible are illustrated by *Figure 6*. This type of column works well only at very low sample to substrate ratios and is necessarily the final step in the scheme.

Gel permeation separation of cyclic hydrocarbons is a relatively new technique (step h). Preliminary runs indicate that a marked enrichment of steranes is possible. The determination of the actual column length and the through put possible are being determined with pure synthetic hydrocarbons. The success of the separation scheme depends on the routine reproducible separation by column chromatography steps. The other operations seem to be rather straightforward.

The state of the experiment is best shown in *Figures 7* and *8*. The major peak in the high resolution capillary chromatogram corresponds to 5α-cholestane and the major fragments in the mass spectrum are consistent. However, there are at least two other higher homologues present. None of the peaks of the gas chromatograms corresponds to known isomers of ergostane or sitostane. Both the 5 α and 5 β isomers of these compounds are widely resolved from 5α-cholestane. The specific rotation of a 2 milligram sample of cholestane isolated by the procedure outlined measured 16 ± 2. The literature value is 24. It is possible that compounds isomeric in the ring skeleton or the side chains are present. Their separation and identification will present a great challenge.

The results, so far, are promising. During the next six months, it is proposed to do the following.. The separations and identifications will be developed into a routine and reproducible

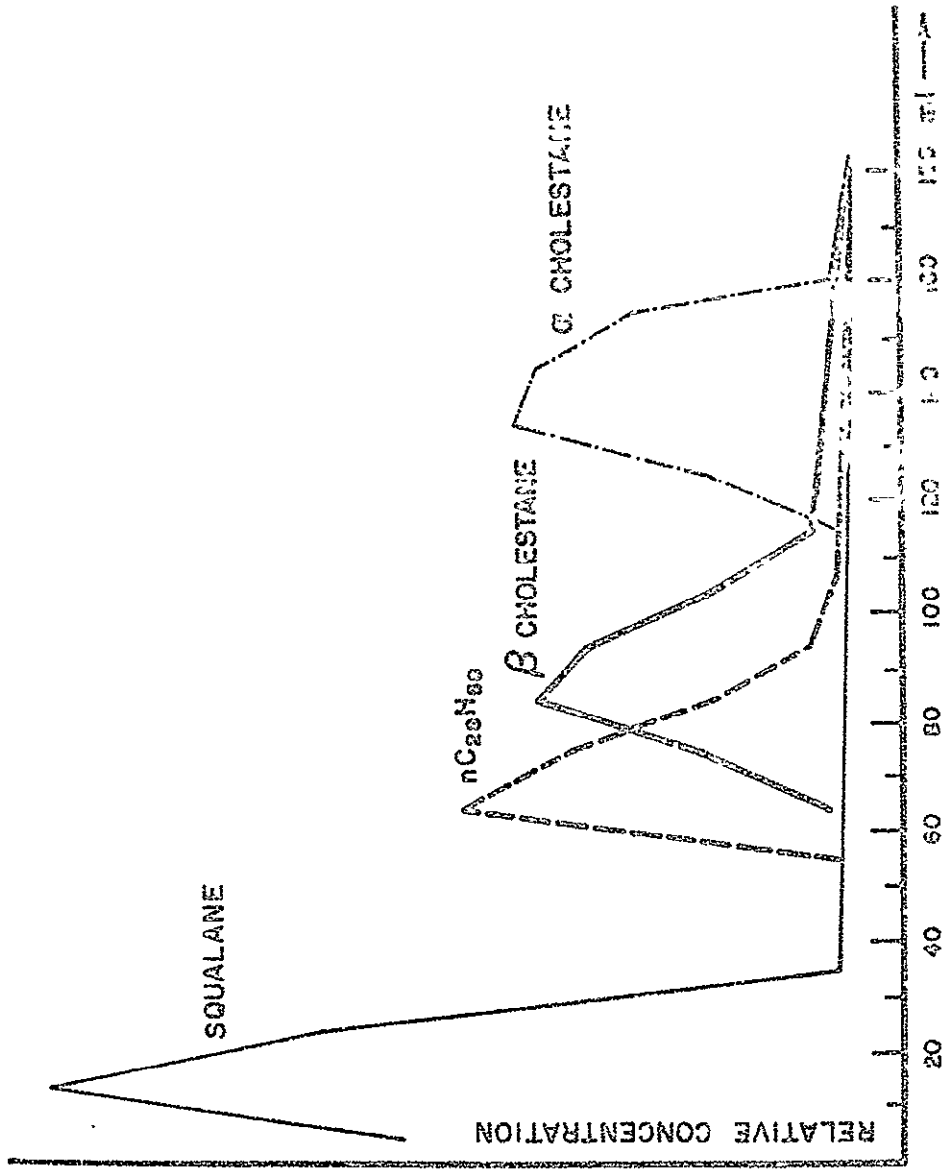

FIGURE 6

Separation of a mixture of normal octacosane, squalane, 5α-cholestane, and 5β-cholestane by alumina chromatography. Twenty milligrams of the mixture in hexane was placed on a dry column of 100 – 200 mesh alumina 25 foot in length and 3/8 inch diameter. The sample was eluted with hexane at a rate of about 1 ml per minute. A pressure of 10 psi was used to force the eluant through the column. Fractions of 10 ml each were collected in an automatic fraction collector. Concentration of each component in the fractions was determined by gas chromatography.

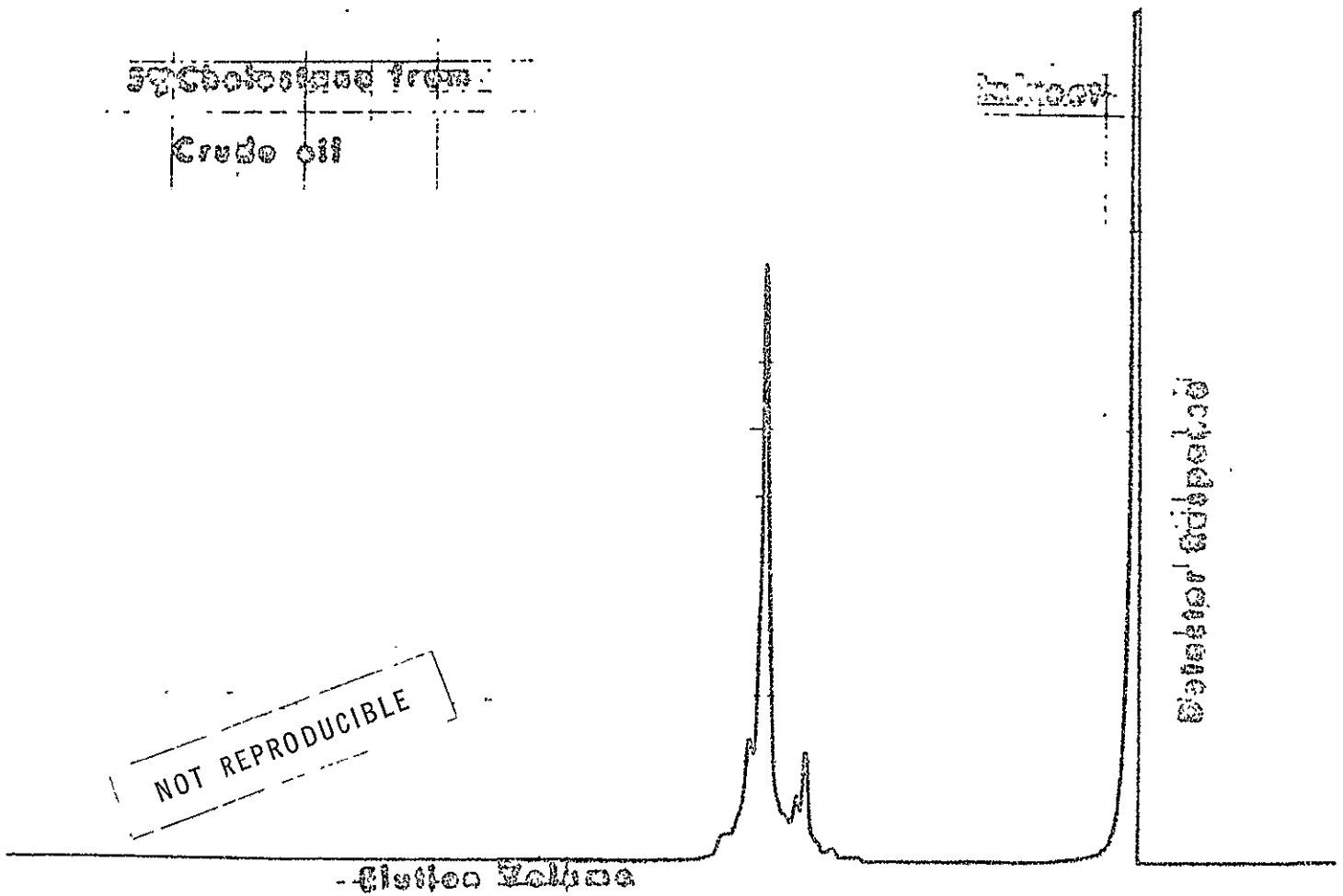

FIGURE 7. Gas chromatogram of 5α-cholestane fraction isolated from crude oil. The separation was made on a Perkin-Elmer 900 gas chromatograph with a 100 foot by 0.010 inch capillary column coated with purified Apiezon L grease. The helium pressure was 30 psi and the column temperature was 300° C.

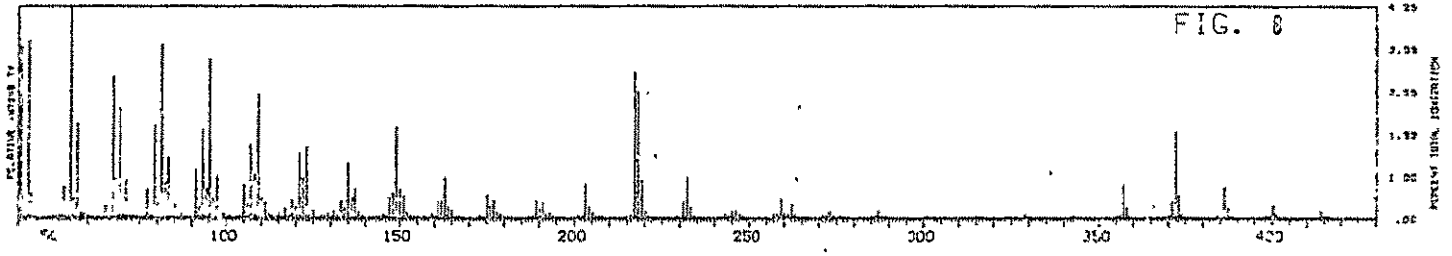

FIGURE 8. Mass spectrum of 5α-cholestane fraction shown in previous figure. Spectrum measured on CEC-110 mass spectrometer at low resolution. Sample introduced on direct insertion probe. Source temperature 220° C. Electron energy, 70 volts.

will be scaled down for smaller sample size. In principle, all of the steps listed will work in the milligram range. As many of the optically active steranes as possible will be identified. High resolution nuclear magnetic resonance may be helpful. The position of the resonance due to the C-19 methyl group has been shown to be dependent on the stereochemistry and substituents of the ring skeleton. A measurement of the optical rotatory dispersion, the variation of optical activity with wave length of the polarized light, would be interesting. All measurements have been made, so far, at the wave length of the sodium D line. Although the dispersion anomaly of saturated hydrocarbons occurs in the vacuum ultraviolet and is inaccessible to commercial instruments, it has been reported that certain high boiling petroleum fraction have a dispersion that is much greater than expected from known steranes. If true, it would make possible the detection of optical activity with a sensitivity an order of magnitude greater than is currently possible.

The necessary pure synthetic compounds needed for this work are not readily available. The synthesis of 5α- and 5β-ergostane and sitostane will be attempted, starting with readily available steroids and using well studied synthetic reactions. A search for steranes with three to six carbon atoms in the side chain at C-17 can be made. The corresponding steroids of living organisms are rare, and this would give information on the transformation of carbon skeletons during the generation and maturation of petroleums.

The high boiling hydrocarbons from the Green River Shale will be isolated and separated. A number of these compounds have been identified in this laboratory the past few years. It is known that triterpanes with 5 rings are present in it. This will give an opportunity to see if the separation scheme can be extended to other hydrocarbon classes.

Green River Formation Oil Shale Bases

The alkanes and carboxylic acids found in the Green River Formation Oil Shale have been discussed in earlier reports. This is to cover the preliminary results of an examination of the bases extracted directly from oil shale both before and after demineralization. Both high and

low resolution mass spectrometry was utilized. *Figure 9* illustrates part of these data, a high resolution spectrum of the total bases isolated from an ether/benzene/methanol extract of this oil shale, and *Figure 10* shows similar data for the total bases isolated from an exhaustive benzene/methanol extract of this shale after demineralization. The spectra obtained at 70 eV, contain both molecular and fragment ions, and an interpretation in terms of the molecular species present can only be tentative.

The exhaustive extract bases were also chromatographed (*Figure 11*) and are to be examined by GC-MS. The most abundant homologous series found are alkyl quinolines (Structure I) or isoquinolines, $C_nH_{2n-11}N$ for $n = 9 - 18$, with $m = 12$ as maximum. This series is also further

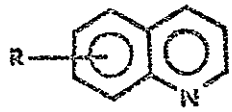

I

R = alkyl

substantiated by the fragment ions due to loss of a methyl radical $C_nH_{2n-12}N$ for $n = 10 - 22$. Alkyl indoles (Structure II), $C_nH_{2n-9}N$ for $n = 8 - 20$ and alkyl pyridines (Structure III), $C_nH_{2n-5}N$ for $n = 6 - 12$ are indicated present in significant quantity by their molecular ions.

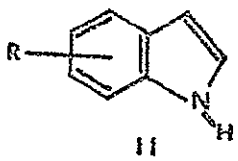

II

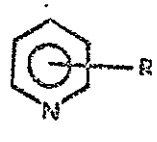

III

R = alkyl

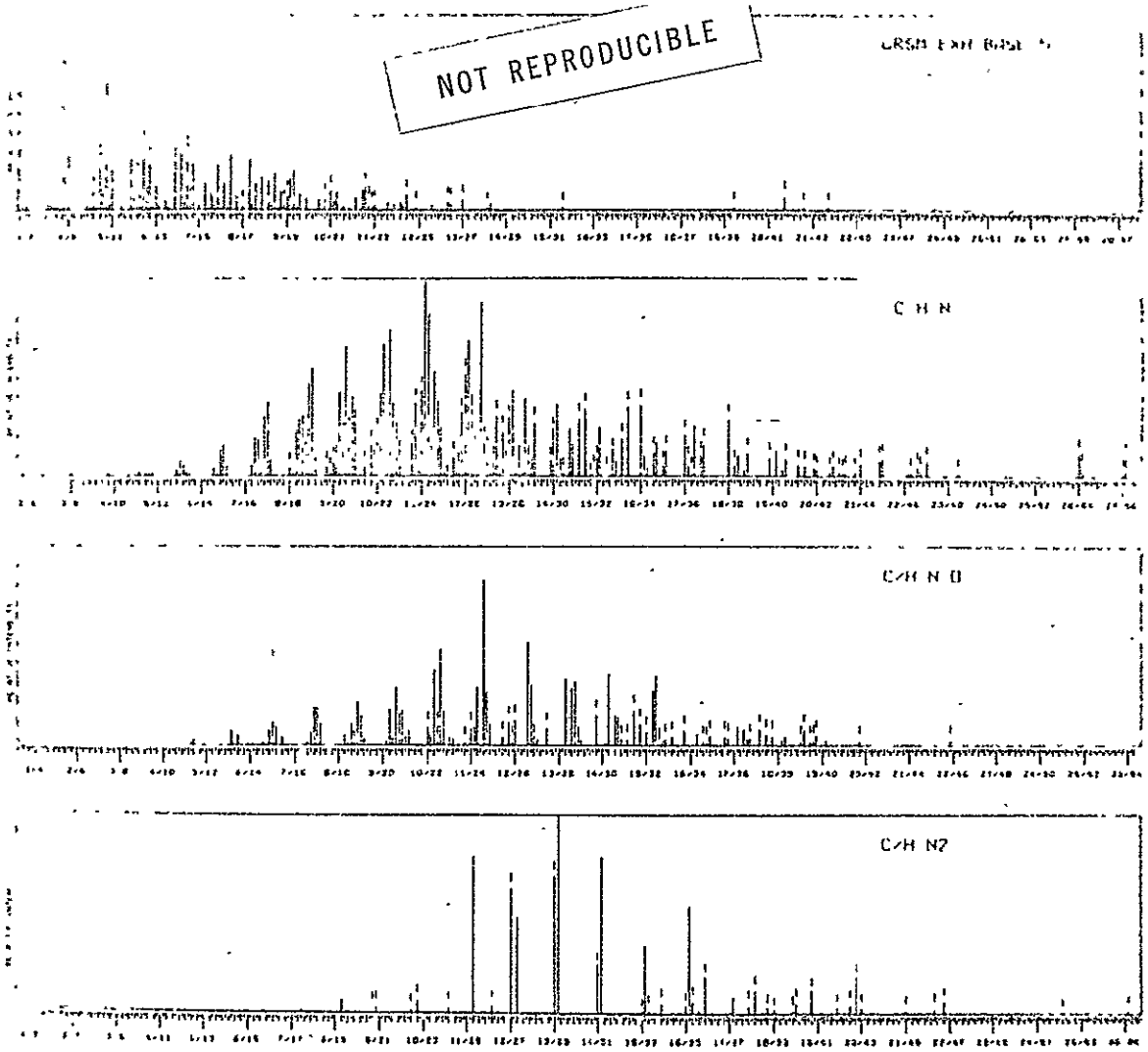

FIGURE 9. The high resolution mass spectrum of the total bases isolated from an exhaustive benzene/methanol extraction of the Green River Formation Oil Shale.

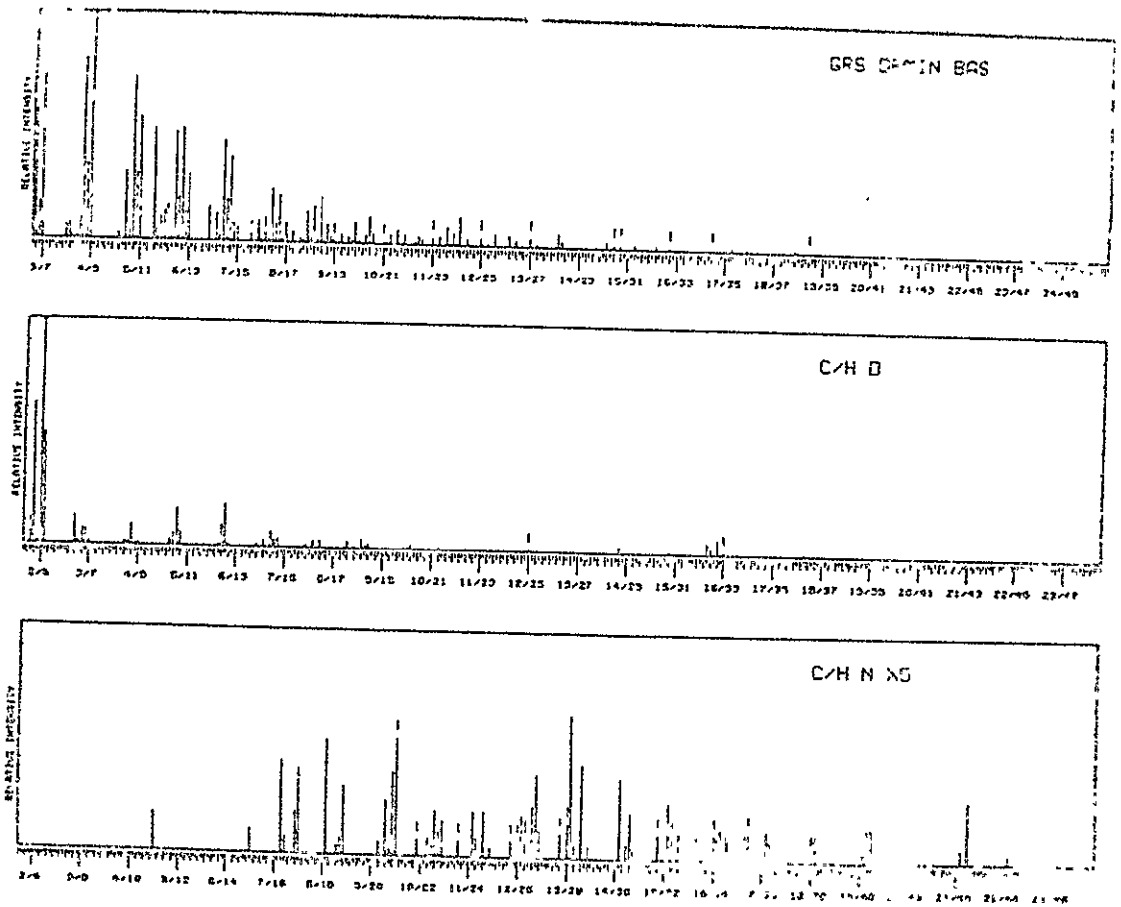

Figure 10. The high resolution mass spectrum of the total base [illegible] the Green River Formation Oil Shale by exhaustive benzene/methanol extraction after demineralization.

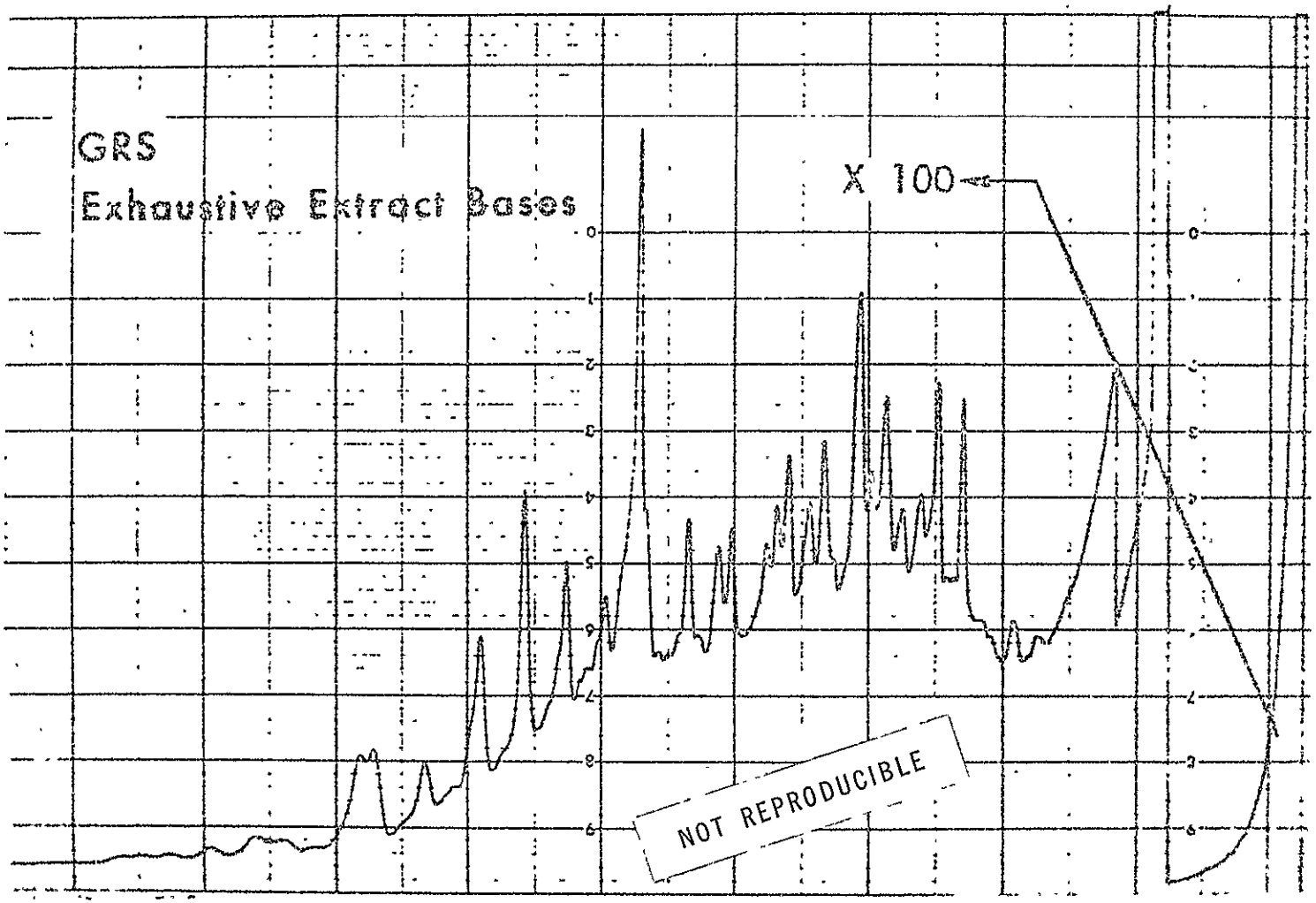

FIGURE 11. The gas chromatogram of the total bases isolated from the Green River Formation Oil Shale by exhaustive benzene/methanol extraction. An Aerograph 204 B gas chromatograph was used with a 5' x 1/8" column of 3% SE – 30 on Gaschrom Z. Temperature programmed, at a rate of 10° C/min. from 100° – 250° C. Helium flow was 30 ml/min.

These two series also show the fragment ions due to H_2 loss $C_nH_{2n-3}N$ for n = 9 – 18 and $C_nH_{2n-6}N$ for n = 6 – 17, respectively. The following homologous series were detected in minor amounts:

a) alkyl tetrahydroquinolines (Structure IV), $C_nH_{2n-7}N$ for n = 8 – 15

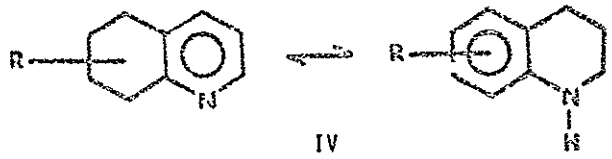

IV

R = alkyl

the fragment ions from loss of CH_3, $C_nH_{2n-8}N$ for n = 8 – 14;

b) alkyl naphthoquinolines (Structure V), $C_nH_{2n-21}N$ for n = 17 – 27 and

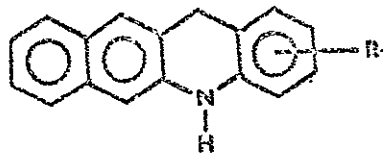

V

R = alkyl

the CH_3 loss fragments, $C_nH_{2n-22}N$ for n = 18 – 22; and

c) alkyl carbazoles (Structure VI), $C_nH_{2n-15}N$ for n = 12 – 14.

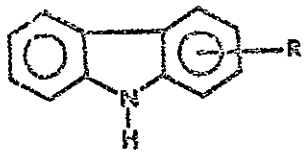

VI

R = alkyl

An interesting group of intense ions can be discerned in the C/H R_2 plot of Figure 9. The homologous series of $C_nH_{2n-10}N_2$ for n = 16 – 18, with n = 14 as maximum can be thought of as breakdown product of porphyrins.

Structure VII can be drawn for n = 14 and Structure VIII for n = 17.

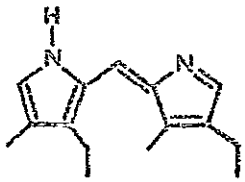

VII

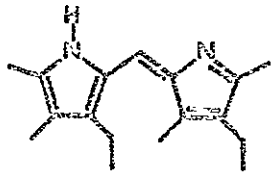

VIII

R = alkyl

These molecular ions are also further substantiated by the series of fragment ions due to CH_3. loss, $C_nH_{2n-11}N_2$ for n = 13 — 17.

The bases isolated from the demineralization extract are a simpler mixture as can be seen from the C/H N plot of Figure 10. Again the major constituent series is the alkyl quinolines (Structure I), $C_nH_{2n-11}N$ for n = 9, 12 — 23. In smaller amounts are found: a) alkyl pyridines (Structure III), $C_nH_{2n-5}N$ for n = 5 — 8; b) alkyl indoles (Structure II), $C_nH_{2n-9}N$ for n = 8, 11, 15, 18, 20, and 22; and c) alkyl tetrahydroquinolines (Structure IV), $C_nH_{2n-7}N$ for n = 9 — 11, 13 and 15.

II. ORGANIC MASS SPECTROMETRY

Detection and Identification of Ketocarboxylic- and Dicarboxylic Acids in Complex Mixtures by Reductive Silylation and Computer-Aided Analysis of High Resolution Mass Spectral Data

Successive solvent extractions of an oil shale from the Green River Formation *(a)* prior to chemical, *(b)* after demineralization with HF/HCl, and *(c)* after chromic acid oxidations of varying duration yield complex mixtures of similar classes of compounds. The acidic fractions of these mixtures were found to consist mainly of aliphatic monocarboxylic and dicarboxylic acids, with aliphatic ketoacids and aromatic carboxylic acids being present in lesser amounts. The presence of the ketoacids was deduced from high resolution mass spectral data determined on the total acid fractions after conversion to methyl esters, in particular by inspection of the pertinent C/H O_3 and C/H O_4 ions.

To confirm the presence of ketoacids independently and, more importantly, to furnish conclusive information regarding the position of the ketofunction within the aliphatic chain, chemical transformation specifically affecting this group was carried out. Reduction of the ester mixture with sodium borohydride (use of sodium borodeuteride would eliminate ambiguities in the case of hydroxy acids originally present in the mixture) resulted in the quantitative conversion of the ketoesters to hydroxy analogs, leaving any diester components unaffected. The hydroxy constituents were then silylated which resulted in greater volatility and a simplified mass spectral fragmentation pattern. In addition, silylation of the hydroxy function introduced a new hetero-atom into structurally significant fragment ions which were unambiguously detected in the high resolution mass spectra and ideally suited for computer search and preinterpretation.

This procedure is well suited for application on a microscale and serves specifically for the detection of ketoacids in the presence of other carboxylic acid constituents. In addition, it yields conclusive structural information regarding the position of the oxofunction. In particular, the suitability of the technique to computer-aided data analysis and interpretation should also permit its useful application to biochemical areas, e.g., lipid analysis of similar complexity.

Further methods of mixture analysis *via* chemical derivatization computer-automated search and preinterpretation are under development.

Ring Contraction in Molecular Ions: Nitrogen-and Oxygen-Containing Systems

The proclivity toward ring enlargement and/or contraction of alicyclic structures is well known from solution chemistry and seems to be paralleled to some degree in mass spectrometric fragmentation. An illustrative example of ring contraction has been encountered in the fragmentation of N-acetylmorpholine,* particularly evident from the rather unusual genesis of M-15 and M-43 ions. While the formation of the first fragment implicates a carbon atom adjacent to nitrogen plus a hydrogen atom

*J. M. Tesarek, W. J. Richter, and A. L. Burlingame, *Org. Mass Spectrom.*, 1, 139 (1968), see preceding semi-annual report.

from the neighboring position, the formation of the latter involves loss of the N-acetyl substituent as a single unit rather than the common two-step loss of hydrogen and ketene:

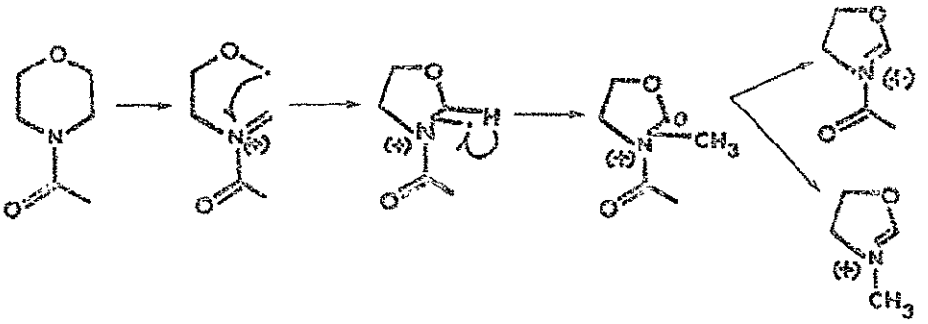

In order to determine effects of modified ring size and omission of the second heteroatom upon ring contraction, a series of related model compounds, mainly N-acetylpyrrolidine, -piperidine, and -hexamethyleneimine, has been studied in this context. The anticipated enhancement of ring contraction with increasing ring size was in fact observed.

Evidently, ring contraction in the smallest member of this series, N-acetylpyrrolidine, is of little significance, because of a strained four-membered cyclic transition state to be traversed. The methyl radical expelled originates exclusively from the acyl substituent rather than the ring moiety, and the loss of C_2H_3O occurs as a two-step process implicating a ring hydrogen atom together with a neutral ketene molecule. In contrast to this behavior, the six-membered homolog, N-acetylpiperidine, decidedly exhibits operation of ring contraction in spite of strong competition from other fragmentation. Analogous contraction, to a six-membered intermediate ion, is observed in N-acetylhexamethyleneimine, as can be concluded from an analysis of the corresponding M-15 and M-43 fragments. Involvement of C-N bond cleavage and loss of an α-carbon atom is deduced for the former fragment from a study of deuterated analogs. The M-43 fragment can be shown to arise from the ejection of the acyl substituent as an intact unit in competition with a two-step alternative.

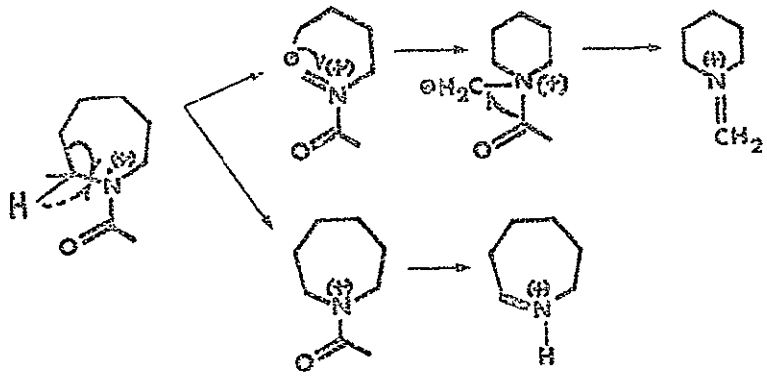

Another obvious extension of these studies concerns similar contraction processes in analogous oxygen-containing heterocycles. Tetrahydropyran, simplest representative of such a series, fails to exhibit a comparable behavior, most probably due to rapid loss of formaldehyde from the molecular ion.* Introduction of a vinylic double bond was employed to circumvent the shortcomings of this model. A more prominent M-15 peak is indeed displayed in the spectrum of 2,3-dihydro-4H-pyran. The importance of this peak is enhanced upon fusion of an aromatic ring to the pyran system. Deuterium labeling of the alicyclic portion of chroman has revealed α-carbon atoms as the primary source of methyl radicals expelled:

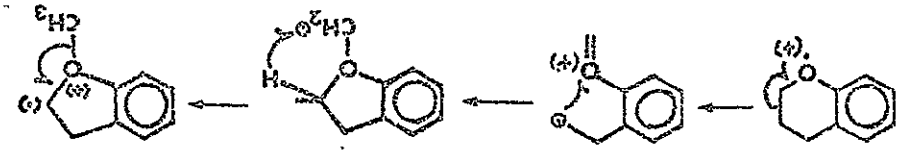

As might be expected, an allylic site of unsaturation, as is present in isochroman, allows excessive formaldehyde loss which renders this isomer incapable of recyclization. However, loss of a methyl radical represents

*R. Smakman and T. J. De Boer, *Org. Mass Spectrom.*, *1*, 403 (1968).

the almost exclusive mode of decomposition in the case of benzoxazepin:

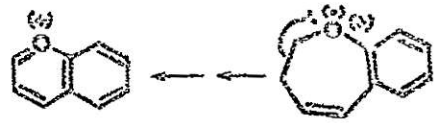

The generation of a highly stablized benzpyrilium ion provides unique driving force for this process.

The rupture of a bond linking carbon to a heteroatom marks an event in fragmentation which is, in principle, conceivable as proceeding through two alternatives of direct cleavage, homolysis, and heterolysis, or through a more complex sequential process, as above. Another example of this latter possiblity is reflected in certain features of the fragmentation of N-acetylpyrrolidine and closely related systems. Contrary to expectations based on the behavior of the free amine, determination of the positional origin of the atoms involved in ejection of ethylene from the molecular ion revealed, in turn, a loss of a carbon atom adjacent to nitrogen:

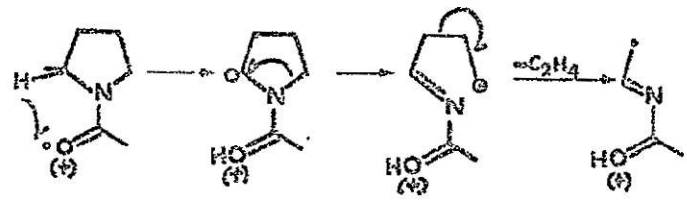

Abstraction of hydrogen from one of the positions adjacent to nitrogen triggers the expulsion of ethylene with rupture of the carbon-nitrogen bond; carbon atoms 2 and 3, with an intact hydrogen environment, are

subsequently expelled, rather than carbon atoms 3 and 4 which would be expected as a result of amine-directed α-cleavage. Operation of a competing amine-directed process can be ascertained only from products of further decomposition; ions resulting from α-cleavage readily fragment further by loss of ketene and hydrogen. Another result of carbonyl-triggered hydrogen abstraction can be seen in the formation of M-1 ions by loss of hydrogen from positions other than those adjacent to nitrogen. The same observations are found to apply to acyl substituents with longer alkyl chains, *i.e.*, N-propionylpyrrolidine and N-n-butyrylpyrrolidine.

Extension of these studies are planned to delineate in more detail the scope as well as the limitations of such fragmentation.

Field Ion Mass Spectrometry

Since the last report, the combined field ionization/electron impact ion source has been improved in several respects. These include the use of electrically etched platinum foil instead of a razor blade as emitter, resulting in larger and more stable ion currents. The sensitivity attainable with the current version is in the range of $10^{-7} - 10^{-6}$ amp/torr with acetone as test gas. The current is measured at the beam monitor of the CEC 21-110 mass spectrometer and pressure determined at the ion source housing. Sensitivity was found to depend strongly upon a parallel alignment of the emitter and the slit in the cathode (repellers). The former experimental layout of the power supplies for field ionization has been rebuilt to allow simple operation of the ion source in either of the modes (field ionization or electron impact) with easy, fast, and convenient change from one mode of operation to the other.

During the course of investigation of the behavior of organic compounds in the field ionization source the following observations have been made. Hydrogen rearrangement is known to be a rather ubiquitous occurence in the organic molecular ions produced in electron impact induced fragmentation. In field ion mass spectrometry, addition or loss of one hydrogen atom, observed only for molecular ions, was shown to result from an interaction with an adsorption layer on the field emitter by intermolecular transfer.

consequently expelled, rather than carbon atoms 3 and 4 which would be expected as a result of amino-directed α-cleavage. Operation of a competing amine-directed process can be ascertained only from products of further decomposition; ions resulting from α-cleavage readily fragment further by loss of ketene and hydrogen. Another result of carbonyl-triggered hydrogen abstraction can be seen in the formation of M-1 ions by loss of hydrogen from positions other than those adjacent to nitrogen. The same observations are found to apply to acyl substituents with longer alkyl chains, i.e., N-propionylpyrrolidine and N-n-butyrylpyrrolidine.

Extension of these studies are planned to delineate in more detail the scope as well as the limitations of such fragmentation.

Field Ion Mass Spectrometry

Since the last report, the combined field ionization/electron impact ion source has been improved in several respects. These include the use of electrically etched platinum foil instead of a razor blade as emitter, resulting in larger and more stable ion currents. The sensitivity attainable with the current version is in the range of $10^{-7} - 10^{-6}$ amp/torr with acetone as test gas. The current is measured at the beam monitor of the CEC 21-110 mass spectrometer and pressure determined at the ion source housing. Sensitivity was found to depend strongly upon a parallel alignment of the emitter and the slit in the cathode (repellers). The former experimental layout of the power supplies for field ionization has been rebuilt to allow simple operation of the ion source in either of the modes (field ionization or electron impact) with easy, fast, and convenient change from one mode of operation to the other.

During the course of investigation of the behavior of organic compounds in the field ionization source the following observations have been made. Hydrogen-rearrangement is known to be a rather ubiquitous occurence in the organic molecular ions produced in electron impact induced fragmentation. In field ion mass spectrometry, addition or loss of one hydrogen atom, observed only for molecular ions, was shown to result from an interaction with an adsorption layer on the field emitter by intermolecular transfer.

Fragmentation due to internal hydrogen rearrangement was claimed to be negligible as a result of rates too low to successfully precede rapid field dissociation ($< 10^{-11}$ sec). Accordingly, the occurrence of such processes was reflected only in the appearance of metastable ions.

Recent studies in our laboratory, however, have shown that hydrogen rearrangement can occur in properly substituted esters to an appreciable extent prior to or concomitant with dissociation. Results demonstrating the degree of specificity of the rearrangement process as well as its dependence on structural prerequisites have been obtained.

III. COMPUTER-COUPLED, LOW RESOLUTION MASS SPECTROMETER SYSTEM

Introduction

This section deals with the development of a computer-coupled, low resolution mass spectrometer system. The system is designed for a preliminary investigation of organic matter in returned samples, from the Apollo program. Presently installed in the Lunar Receiving Laboratory at the Manned Spacecraft Center in Houston, this system has been developed in collaboration with Dr. K. Biemann at the Massachusetts Institute of Technology. The M.I.T. Group has responsibility for the development of the mass spectrometer and associated sample introduction systems. Dr. A. L. Burlingame has responsibility for the development of the computer system and programming for data acquisition and reduction.

Hardware

The computer system and associated peripheral equipment were discussed in the previous semi-annual report. This system is essentially complete. System #1 has been shipped to M.I.T. and tested with a duplicate of the mass spectrometer system. These tests resulted in several changes in the various programs for data reduction, and indicated the necessity for a few minor changes in the methods of scan control and MS-computer interfacing. In general, these preliminary tests were quite successful, and indicated that the experiment as conceived could be carried out successfully without any major changes in either the computer or mass spectrometer hardware.

System #1 was shipped to LRL in Houston shortly before February 1. The computer itself survived all its travels quite well. The magnetic tape unit arrived in Houston with some minor problems, most of which have been taken care of. By March 4 the unit will be completely operational. The modifications to this system as it presently exists include the following: 1) addition of a scan control clock system for regulation of both the up and down scan times; 2) modification to the mass spectrometer scan rates; 3) addition of analog circuitry for automatic measurement of critical temperatures in the inlet system; 4) addition of two more interrupt levels to the computer; 5) upgrading of some digital circuitry in the various peripheral equipment interfacing.

The CRT display is scheduled for installation and testing within the week, thus completing the hardware at LRL. Other minor changes in the hardware will probably take place based on the results of the March simulation, at LRL.

Software

The programming for this system is usable at this time. Several new programs are scheduled for completion within the week to simplify the task of data reduction and presentation.

The data acquisition programs are based on a controlled, repetitive scan on the mass spectrometer. Data are acquired and handled during an exponential down-scan of the mass spectrometer. The methods in which the data are handled depend on the operator's discretion and the particular experiment being carried out.

The techniques for data reduction are derived from two sources. The first source is the techniques used in our present programming for data reduction of high resolution mass spectra. From this source the methods of instrument mass *vs.* time calibration and subsequent mass calculation are derived. The second source is the techniques used in data reduction from a low resolution mass spectrometer-computer system similar in many respects to the system at LRL, but employing different mass spectrometers.

The combination of these techniques has led to development of an operational data reduction system that works with the Hitachi RMU-6 Mass Spectrometer, using either a hydrocarbon or perfluorokerosene as a mass calibration standard. Also in the data reduction package are routines for plotting and displaying mass spectra and routines for searching data tapes for various spectra and summarizing the results of an analysis.

This system will undergo a full-scale test during March simulation at LRL. Any changes necessary in hardware or software as dictated by the results of the simulation will be made during or immediately after the month of March.

IV. LUNAR MODULE DESCENT ENGINE EXHAUST GAS SAMPLING PROGRAM

The High Resolution Mass Spectral Analyses of Background and Firings

The Lunar Module Descent Engine Exhaust Gas Sampling Program was devised to analyze the organic combustion products generated by the Lunar Module Descent Engine. From a cosmo- and geochemical viewpoint, the carbonaceous compounds of higher molecular weight were of particular interest. A sampling system consisting of four traps ranging from ambient to liquid nitrogen temperatures (Trap A:— ambient, Trap B: — 20°C Trap C: — 79°C and Trap D: — 196°C) was built at NASA White Sands Test Facility. The schematic of this sampling system is illustrated in *Figure 12*. For Phase I of the program a model engine (5 lb thrust) was constructed and fired to obtain preliminary experience with the collecting system and also to evaluate the background. The schematic of the model engine and sampling probe is illustrated in *Figure 13* and a perspective drawing in *Figure 14*.

For Phase II of the program the sampling system was installed as indicated in *Figure 15* to sample the LM descent engine exhaust (WSTF Test Stand 401). The test stand is 32 × 25 feet with all surfaces contaminated by paints, oils, etc. The operating pressures range from 10^{-2} torr to 1 torr according to the leak rate into the system. The chamber is roughed down with a cam and piston roughing pump, followed

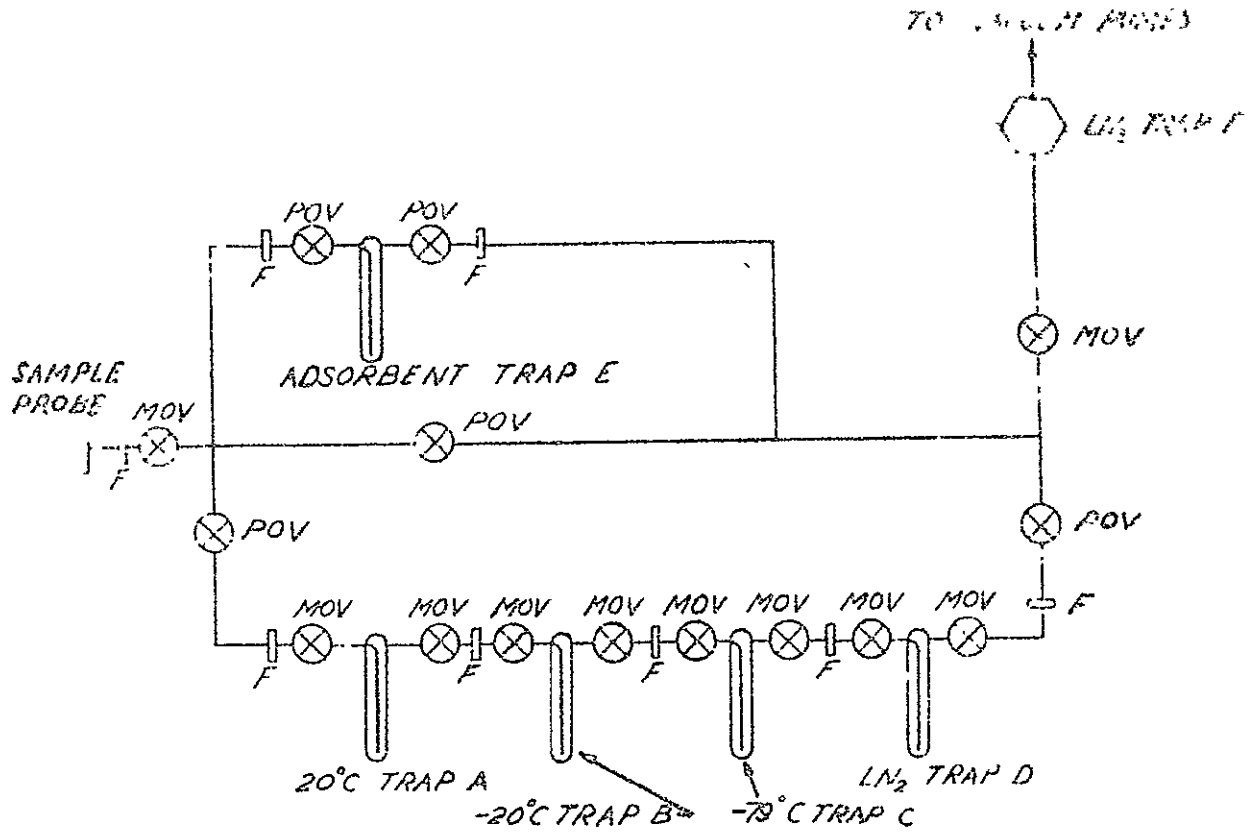

FIGURE 12. Traps A thru D — 1.5 in. inner tube, 3.0 in. outer tube, 15 in. length, glass wool filled.

Trap E — Adsorbent filled 1.5 in. inner tube, 3.0 in. outer tube, 15 in. length.

Trap F — Granville-Phillips 2 in. trap, or equal.

POV — Pneumatic operated valve, $1\frac{1}{2}$ in. Ultek Model 40 471, or equal.

MOV — Manually operated valve, Varian Conflat Model 951-0023, $1\frac{1}{2}$ in., or equal.

F — Flange, $2\frac{3}{4} \times 1\frac{1}{2}$ Varian Conflat Model 954-5071, or equal.

All tubing 1.5 in. 304 SS.
All Weldments TIG.

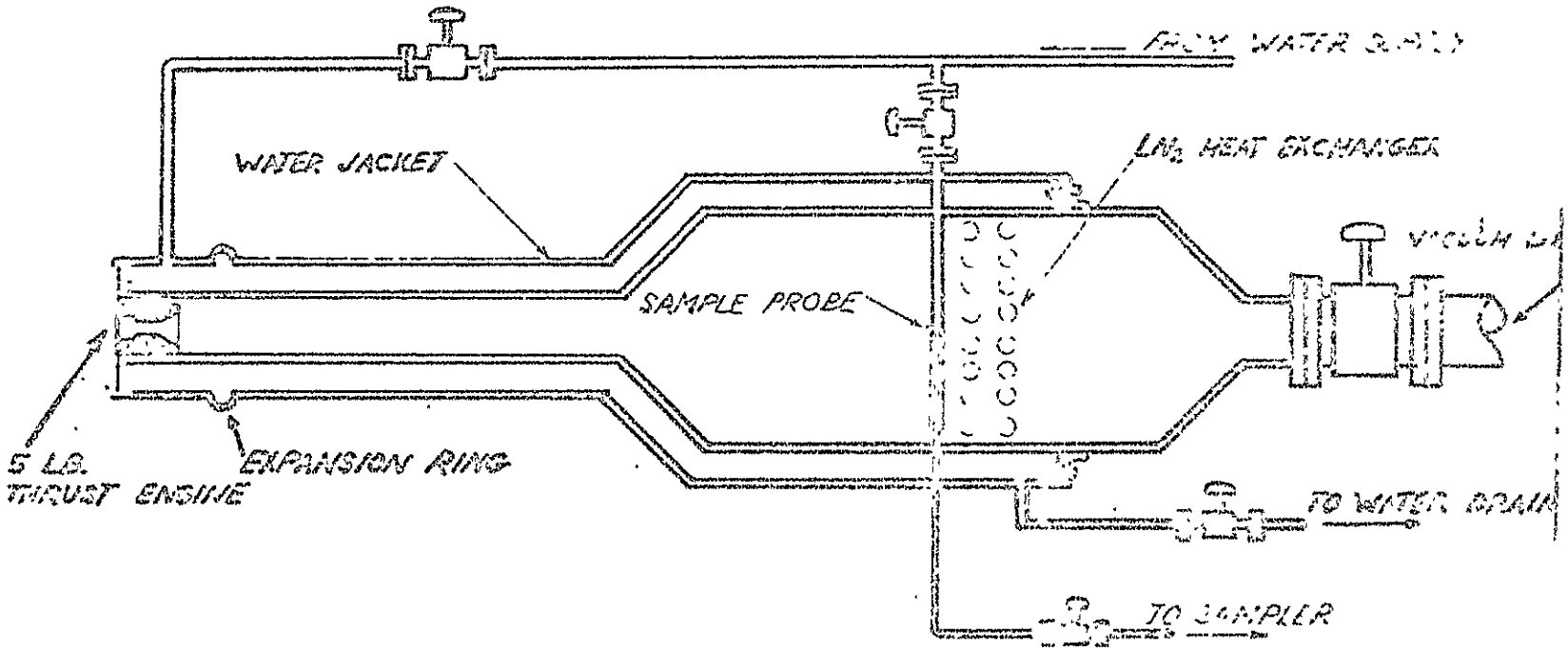

FIGURE 13
VACUUM CHAMBER LAYOUT

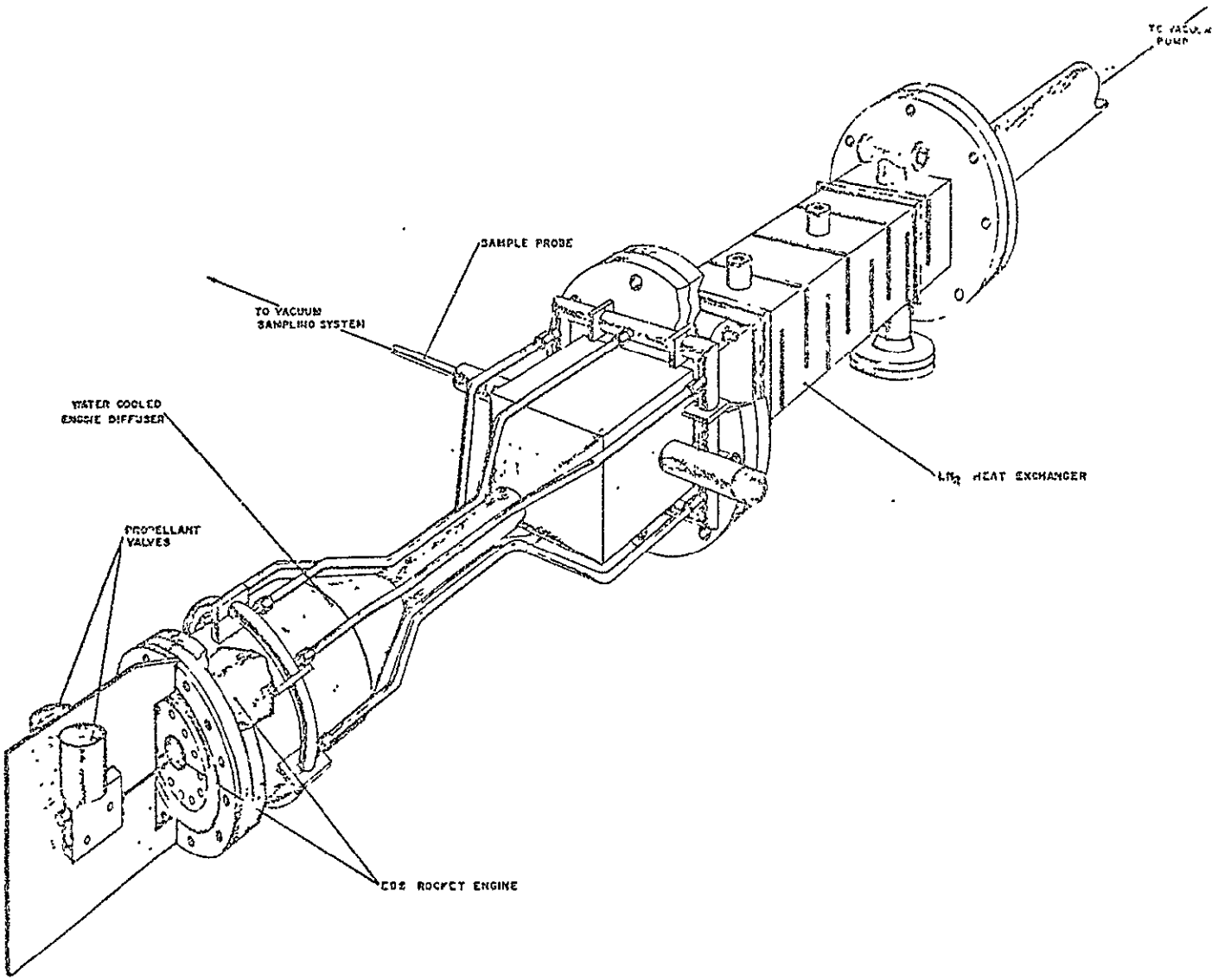

FIGURE 14. Mode engine and sample probe.

FIGURE 15
PHASE II TEST FACILITY

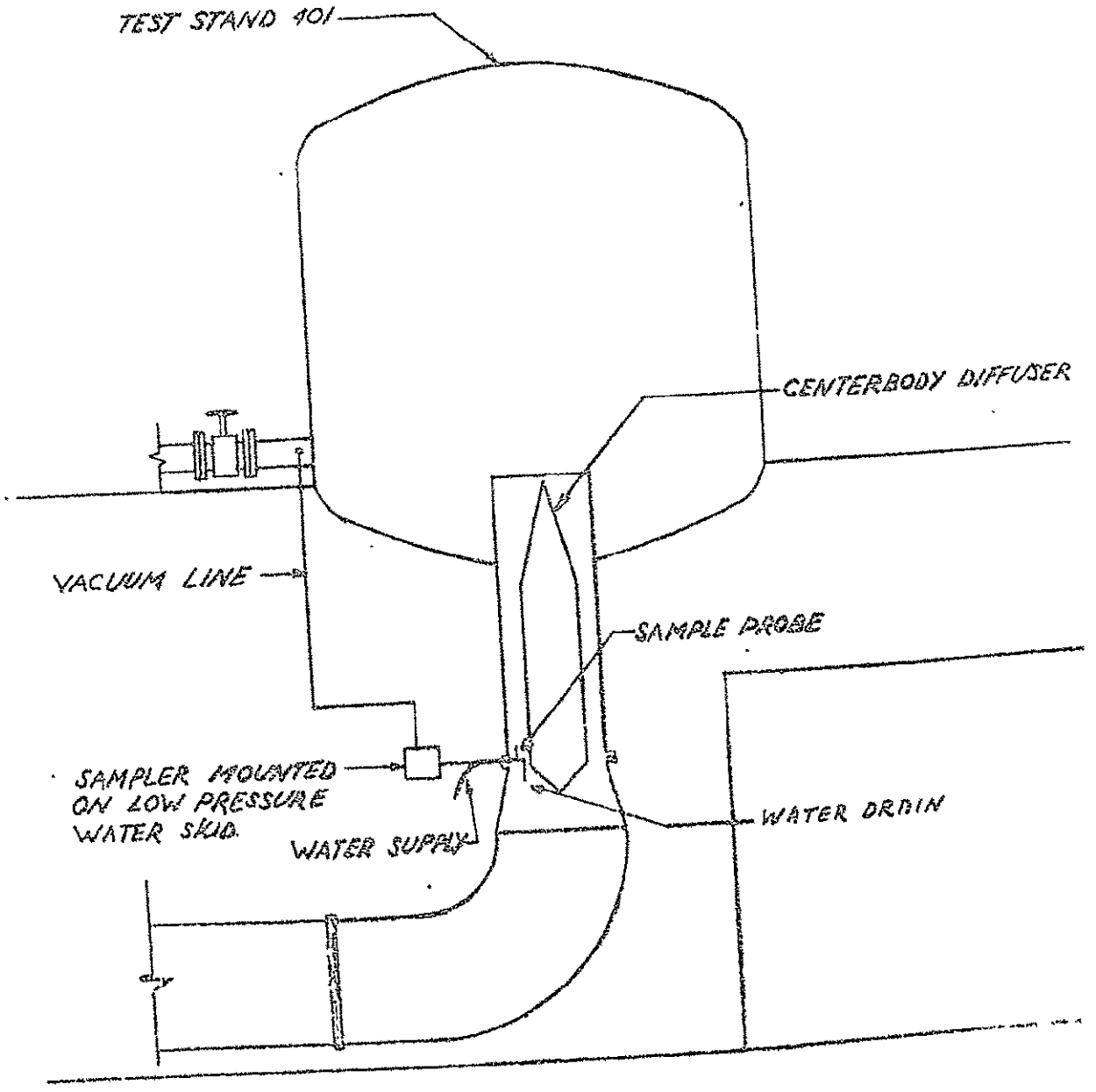

by a positive displacement, lobe-type blower. Just before ignition of the engine the high pressure steam vacuum system takes over. The sample probe (1/2" diam.) protrudes 6" into the center body diffuser section of the steam ejector.

Samples

The following samples sets (Traps A, B, C, and D per set) were received at the Space Sciences Laboratory, University of California, Berkeley:

a) Phase I (Series IV, Test 002) Model engine background. Here the sampling system was purged with gaseous nitrogen during a 600 second sampling.

b) Phase I (Series IV, Test 003) Model firing. The trapping system was at 31 microns pressure initially and 83 microns at the end of the run. The sampling was for 25 seconds duration.

c) Phase II (Series V, Test 002) LM engine firing, 100% full thrust Collection for 25 seconds at full thrust. (The pressures in the traps after a firing (before shipment) were approximately: A. 64 torr, B. 102 torr, C. 191 torr, and D. 2 lbs [gauge].)

d) Phase II (Series V, Test 003) LM engine, firing, 28 — 33% full thrust. Collection for 50 seconds at that thrust. Traps had been through new, recommended cleaning procedure.

e) Phase II (Series V, Test 004) LM engine firing, 500 second collection at the firing profile:

% Full Thrust	Time (sec)
100	0 — 305
54 — 42 (ramp)	305 — 403
40	403 — 425
40 — 32 (ramp)	425 — 500

The traps were cleaned by the new recommended procedure. An additional trap (E) was used to collect exhaust gas products at — 320°F using no glass wool as collection barrier.

Trapped Volatile Gases

The volatile gases in the three sets of traps were analyzed by high resolution mass spectrometry. The samples were introduced via a gas sample doser into a GEC-AEI MS-902 Mass Spectrometer and run on-line to an SDS Sigma 7 Computer. The resolution was 10,000, ionizing potential 70 ev, and ion source temperature 240°C.

All traps of Phase I, Series IV, Tests 002 and 003 and Phase II, Series V, Tests 002 and 003 were found to contain mostly air at rather high pressure. This was assumed to be leakage during shipment and subsequent storage, since the N_2 and O_2 peaks in all mass spectra had the same intensity ratios (the D traps, lN_2 cooled, should have a higher O_2 content if the air were in the sampling system). An example of a high resolution mass spectrum listing is found in Table I.

Trap Washings (Nonvolatiles)

The traps were then vented to atmosphere and solvent was extracted. The side valve was fully opened and 1 liter 3:1 benzene/methanol (distilled or nano-grade) poured in. The trap was shaken and allowed to soak for about 5 minutes, then it was turned upside down to drain out the solvent mixture. Usually 300 — 500 ml was recovered (the remainder was held up by the glass wool), approx. 50% extraction efficiency. The extracts were concentrated under vacuum using a Büchi evaporator and weighed after all solvent was removed (the weights are listed in Table II).

Mass Spectrometry Results

The high resolution mass spectra were determined for all extracts using a GEC-AEI MS-902 Mass Spectrometer on-line to an SDS Sigma 7 Computer. The samples were introduced directly into the ion source by means of a D.I. probe, and consecutive scans were taken at increasing ion source temperatures to insure complete sample volatilization. The operating resolution was 10,000, ionizing current 70 ev, and source temperature 190 — 270°C. The findings are discussed in a later section and the

TABLE I

PLAL DATA 130 LEM MOD TRAP D VOLAT SCAN 1 135072.00

MASS	TIME	INTENSITY	OBS MASS	TRUE MASS	DIFFERENCE	C	H	N	O	
15	55440.00	31	15.0130980	15.0108978	-.0022002	0	1	1	0	
26	159493.09	127	26.0152020	26.0156492	.0004472	2	2	0	0	— HC≡CH
27	166680.84	99	27.0234059	27.0234738	.0000679	2	3	0	0	
28	173357.20	1302	27.9949985	27.9949141	-.0000844	1	0	0	1	— CO
28	173432.47	16287	28.0061500	28.0061464	-.0000036	0	0	2	0	— N_2
28	173604.00	35	28.0315794	28.0312984	-.0002810	2	4	0	0	— CH_2-CH_2
29	180043.34	219	29.0031744	29.0027387	-.0004357	1	1	0	1	— HC = O
32	198564.31	2974	31.9903809	31.9898282	-.0005527	0	0	0	2	— O_2
39	236089.35	68	39.0239001	39.0234738	-.0004263	3	3	0	0	
41	245592.54	105	41.0393251	41.0391230	-.0002021	3	5	0	0	
44	258593.54	698	43.9902881	43.9898282	-.0004599	1	0	0	2	— CO_2
55	300939.95	62	55.0559304	55.0547722	-.0011582	4	7	0	0	
56	304416.35	45	56.0631495	56.0625968	-.0005527	4	8	0	0	
57	307770.50	23	57.0699881	57.0704214	.0004333	4	9	0	0	

Table II Trap Extract Weights (in mg)

Trap	A	B	C	D
Model Background (600 sec.)	6.3	39.2	4.6	5.8
Model Firing (25 sec.)	5.1	7.4	8.2	22.7
LM Engine Firing (25 sec.)	13.7	10.6	8.3	18.4
Cleaned & Baked Out			10.6	
LM Engine Firing (50 sec.)	5.1	0.8	0.5	lost in sampling

organics thought to originate from engine combustion products are tabulated in Table III.

The major constituents of the background are hydrocarbons, both aliphatics and aromatics, ranging from low molecular weight to ~ C$_{35}$. Oxygenated species such as aliphatic ketones and acids are also found. Substantial quantities of silicone oil and "octoil" (phthalate esters) are found in the extracts.

It should be pointed out that the trapping system had been used to collect several sets of firing samples before this background collection was made. Thus, significant quantities of nitrogenous products formed by the combustion are found in the trap extracts.

An example of the high resolution mass spectral data of a background extract (Trap C Model Background — 600 cec) is shown in *Figure 16*, a peak at m/e 167, $C_8H_7O_4$ and a peak at m/e 279, $C_{16}H_{23}O_4$ (structure I).

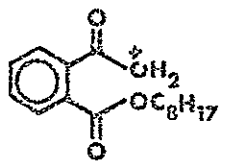

I

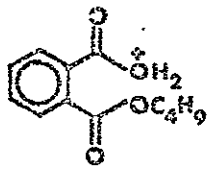

II

Dibutylphthalate is also present as discerned from peaks at m/e 205, $C_{12}H_{13}O_3$ (C/H O_3 plot of Fig. 16) and m/e 223, $C_{12}H_{15}O_4$ (structure II). The heptane insoluble portion of the background trap B extract was analyzed by IR spectrometry and found to be identical to silicone pump oil (done at NASA — White Sands T.F.). In the high resolution mass spectral data the characteristic triplets of the silicon isotopes were detected for a series of ions of structures: III, n = 0 — 3, IV, n = 2 and 3; and V, n = 0 and 1.

TABLE III. A SUMMARY OF LH ROCKET COMBUSTION PRODUCTS FOUND BY HIGH RESOLUTION MASS SPECTROMETRY (LISTED AS ION COMPOSITIONS)

M/E	STRUCTURE OF ION	MODEL	ENGINE	PLOT REFERENCE
26	CH	+	+	C/H N Fig. 17 & 19
	$HC \equiv CH$	+	+	C/H Fig. 17 & 19
27	HCN	+	+	C/H N Fig. 17 & 19
	$H_2C = \dot{C}H$	+	+	C/H Fig. 17 & 19
28	CO	+	+	C/H O Fig. 17 & 19
	N_2	+	+	
	$CH_2 = N\cdot$	+	+	C/H N Fig. 17 & 19
	$CH_2 = CH_2$	+	+	C/H Fig. 17 & 19
29		+	+	C/H O Fig. 17 & 19
	$CH_3 - CH_2\cdot$	+	+	C/H Fig. 17 & 19
30	NO	+	+	C/H NO Fig. 17 & 19
	$CH_2 = O$	+	+	C/H O Fig. 17 & 19
	$CH_2 = \dot{N}H_2$	+	+	C/H N Fig. 17 & 19
31	$CH_3O\cdot$	+	+	C/H O Fig, 17, 18 & 19
32	O_2	+	+	C/H O_2 Fig. 17, 18 & 19
	CH_3OH	+	+	C/H O Fig. 17, 18 & 19
38	C_3H_2	+	+	C/H Fig. 17, 18 & 19
39	C_3H_3	+	+	C/H Fig. 17, 18 & 19
40	C_3H_4	+	+	C/H Fig. 17, 18 & 19
41	$HC \equiv C - O\cdot$	+	+	C/H O Fig. 17, 18 & 19
	C_2H_3N	+	+	C/H N Fig. 17, 18 & 19
	C_3H_5	+	+	C/H Fig. 17, 18 & 19

M/E	STRUCTURE OF ION	MODEL	ENGINE	PLOT REFERENCE
42	$CH_2 = C = O$	+	+	C/H O Fig. 17, 18 & 19
	$CH_2 = \overset{+}{N} = CH_2$	+	+	C/H N Fig. 17, 18 & 19
	$CH_3 - CH = CH_2$	+	+	C/H Fig. 17, 18 & 19
43	HCNO	+		C/H NO Fig. 17, 18 & 19
	$CH_3 - C \equiv O$	+	+	C/H O Fig. 17, 18 & 19
	$CH_3 - N = CH_2$	+	+	C/H N Fig. 17, 18 & 19
	$CH_3CH_2CH_2^{\cdot}$	+	+	C/H Fig. 17, 18 & 19
44	CO_2	+	+	C/H O_2 Fig. 17, 18 & 19
	H_2CNO	+	+	C/H NO Fig. 17, 18 & 19
	$CH_3CH = O$	+	+	C/H O Fig. 17, 18 & 19
	$CH_3 - N = NH$	+	+	C/H N_2 Fig. 18
	$CH_3 - N - CH_3$	+	+	C/H N Fig. 17, 18 & 19
45	CO_2H^+	+	+	C/H O_2 Fig. 17, 18 & 19
	CH_3NO	+		C/H NO Fig. 17, 18 & 19
46	NO_2	+		C/H NO_2 Fig. 17 & 18
	HCO_2H	+	+	C/H O_2 Fig. 17, 18 & 19
47	HNO_2	+		C/H NO_2 Fig. 17 & 18
50-55		+	+	C/H Fig. 17, 18 & 19
55	$CH_2 = CH - C \equiv O^+$	+	+	C/H O Fig. 17, 18 & 19
56	$CH_3\overset{+}{N}H_2 - C \equiv CH$	+	+	C/H N Fig. 17, 18 & 19
		+	+	C/H Fig. 17, 18 & 19
57	$CH_3C = OCH_2^{\cdot}$	+	+	C/H O Fig. 17, 18 & 19
		+	+	C/H Fig. 17, 18 & 19

M/E	STRUCTURE OF ION	MODEL	ENGINE	PLOT REFERENCE
58	CH_3COCH_3	+	+	C/H O Fig. 17, 18 & 19
	$(CH_3)_2\overset{+}{N}=CH_2$	+		C/H N Fig. 17, 18 & 19
59	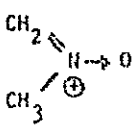	+	+	C/H NO Fig. 17, 18 & 19
	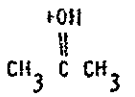	+	+	C/H O Fig. 17, 18 & 19
60	CH_3CO_2H	+	+	C/H O_2 Fig. 17 & 18
	$CH_3NH-N=O$	+	+	C/H N_2O Fig. 17 & 18
	$(CH_3)_2\overset{+}{N}=O$	+	+	C/H NO Fig. 17, 18 & 19
61	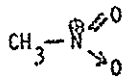	+		C/H NO_2 Fig. 17 & 18
	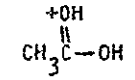	+	+	C/H O_2 Fig. 17, 18 & 19
67	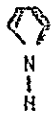	+		C/H N Fig. 17 & 18
70	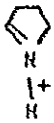	+		C/H N Fig. 17 & 18
72	C_3H_6NO		+	C/H NO Fig. 17, 18 & 19
73	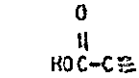	+	+	C/H O_3 Fig. 17, 18 & 19
	$CH_3CH_2CO_2^{\cdot}$	+	+	C/H O_2 Fig. 17, 18 & 19
76-84	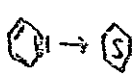	+	+	C/H Fig. 17, 18 & 19

M/E	STRUCTURE OF ION	MODEL	ENGINE	PLOT REFERENCE
85	C_4H_6NO		+	C/H N_2 Fig. 17, 18 & 19
88	$C_4H_8O_2$	+	+	C/H O_2 Fig. 17, 18 & 19
91-93	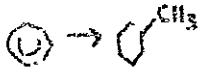	+	+	C/H Fig. 17, 18 & 19

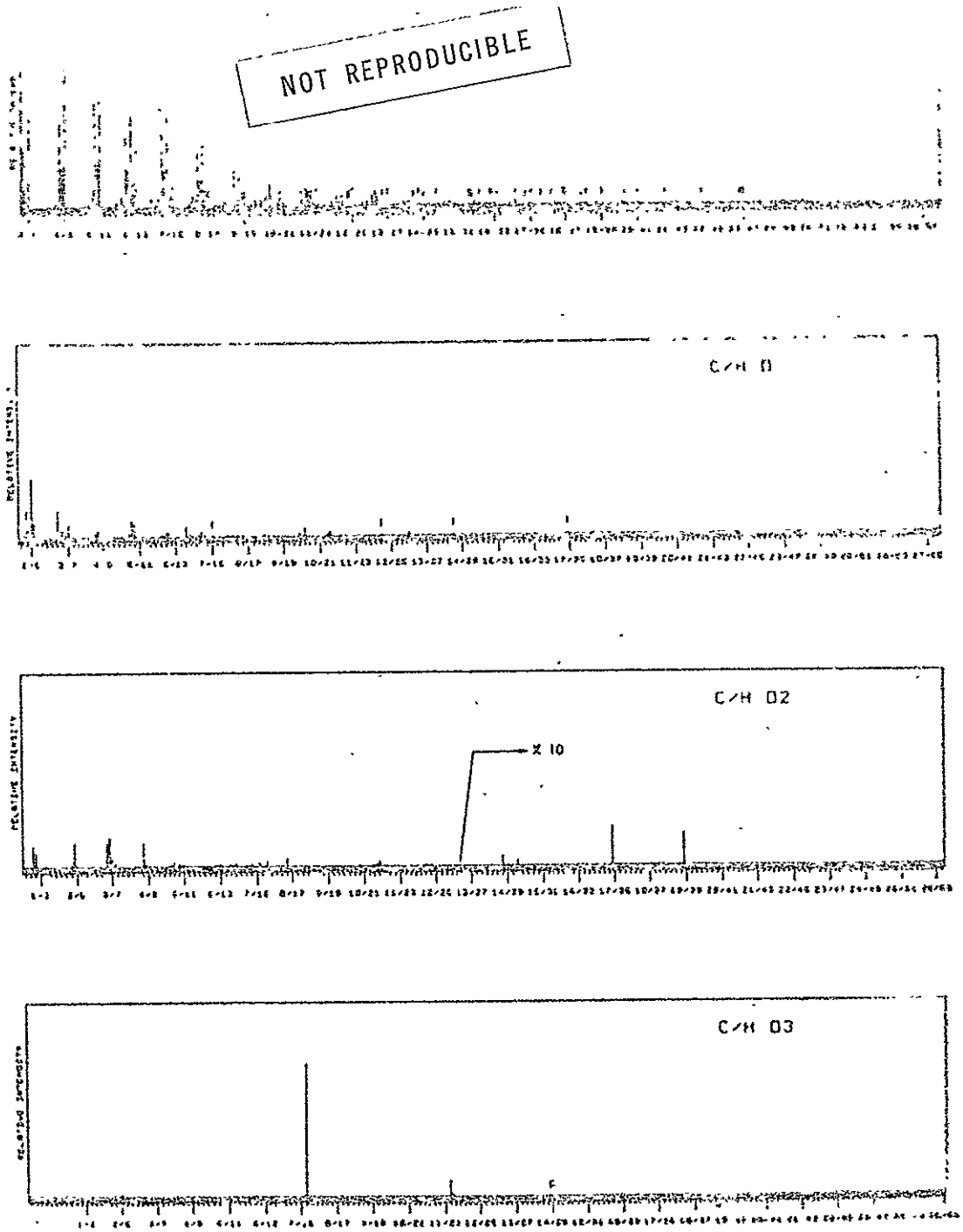

FIGURE 16. The high resolution mass spectrum of a background extract (Trap C Model Background – 600 sec).

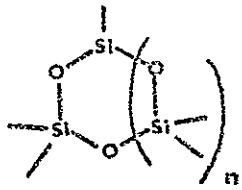

III

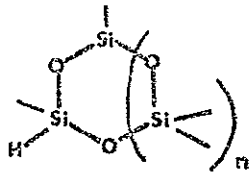

IV

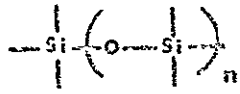

V

The aliphatic hydrocarbon pattern is established from the exponential decrease of the fragment ion intensities of the homologous series: C_nH_{2n+1}, ranging from n = 3 — 23$^+$ and C_nH_{2n-1}, ranging from n = 3 — 20$^+$ (C/H plot of Fig. 16). The former homologs are fragments of saturated hydrocarbons and the latter are homologs of olefinic and/or cyclic hydrocarbons. There are small quantities of ketonic and carboxylic acid components present. Ketones, $C_nH_{2n}O$, ranging from n = 2 — 4 and $C_nH_{2n-2}O$, ranging from n = 2 — 7 (C/H O plot of Fig. 16) and acids, $C_nH_{2n-2}O_2$, ranging from n = 2 — 6 (C/H O_2 plot of Fig. 16) are indicated in the spectra. At the higher mass end of the C/H O_2 plot of Fig. 16 two peaks are indicated: $C_{17}H_{34}O_2$ and $C_{19}H_{38}O_2$. These are thought to be methyl palmitate and methyl stearate, since there is a significant peak at m/e 74, $C_3H_6O_2$, the McLafferty rearrangement of methyl esters.

The samples of trap extract from the firing of the model engine are for the most part background with some superimposed combustion products. Two examples are used as illustrations. *Figure 17a* and *b* presents the high resolution mass spectral data for the extract of trap C and *Figure 18a* and *b* shows similar data for trap D.

The background is still present as, for example, octoil (m/e 149, $C_8H_5O_3$ in the C/H O_3 of Figs. 17a and 18a) and the hydrocarbon pattern (cf. C/H plots of Figs. 16, 17a, and 18a). The lower molecular weight combustion products of unsymm-Dimethylhydrazine (UDMH) and N_2O_4 can be identified in the high resolution mass spectra among the background, and they are listed in Table III. The intensities indicated in the figures

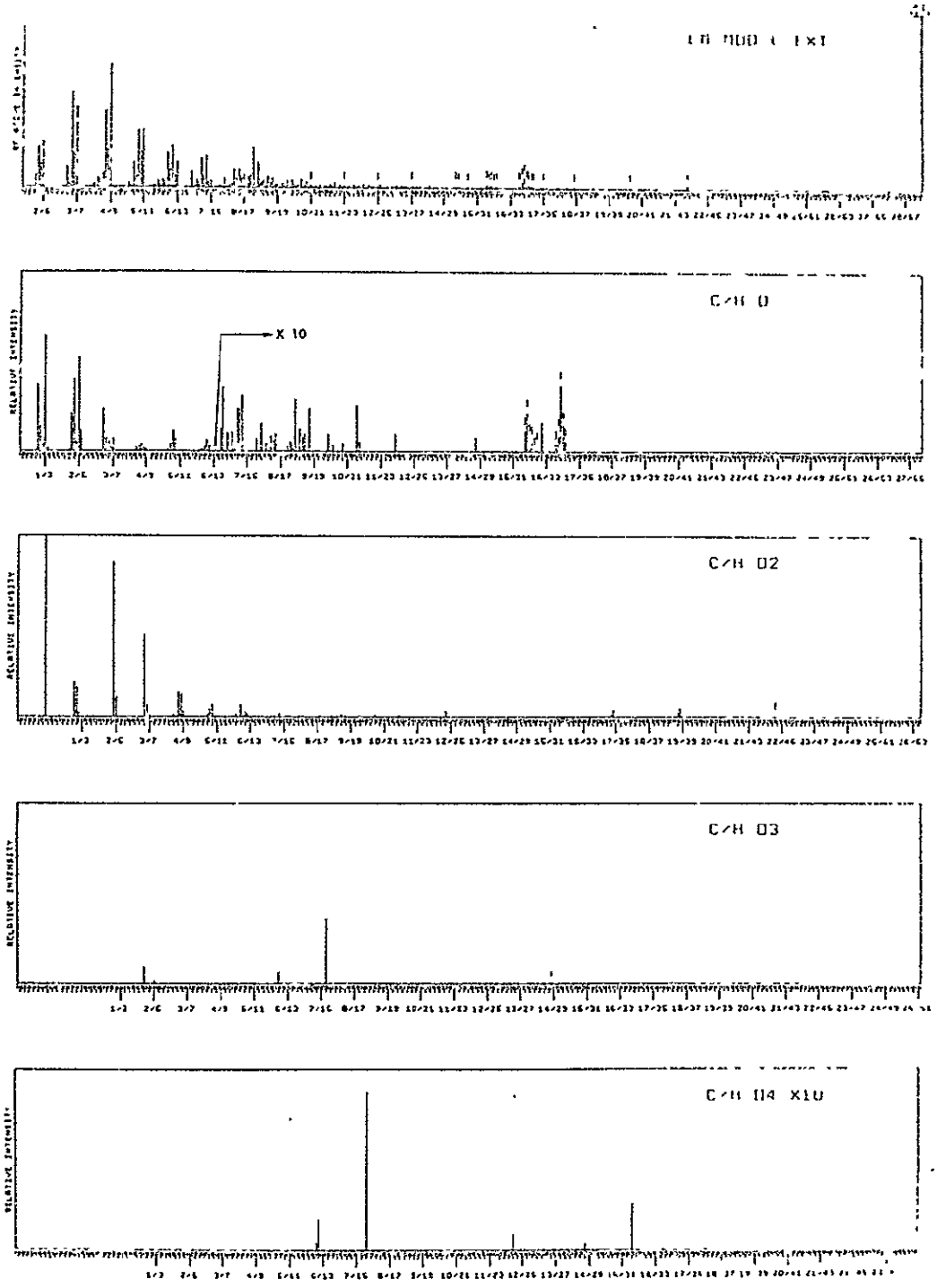

FIGURE 17-a. The partial high resolution mass spectrum of the Trap C extract from the model engine firing.

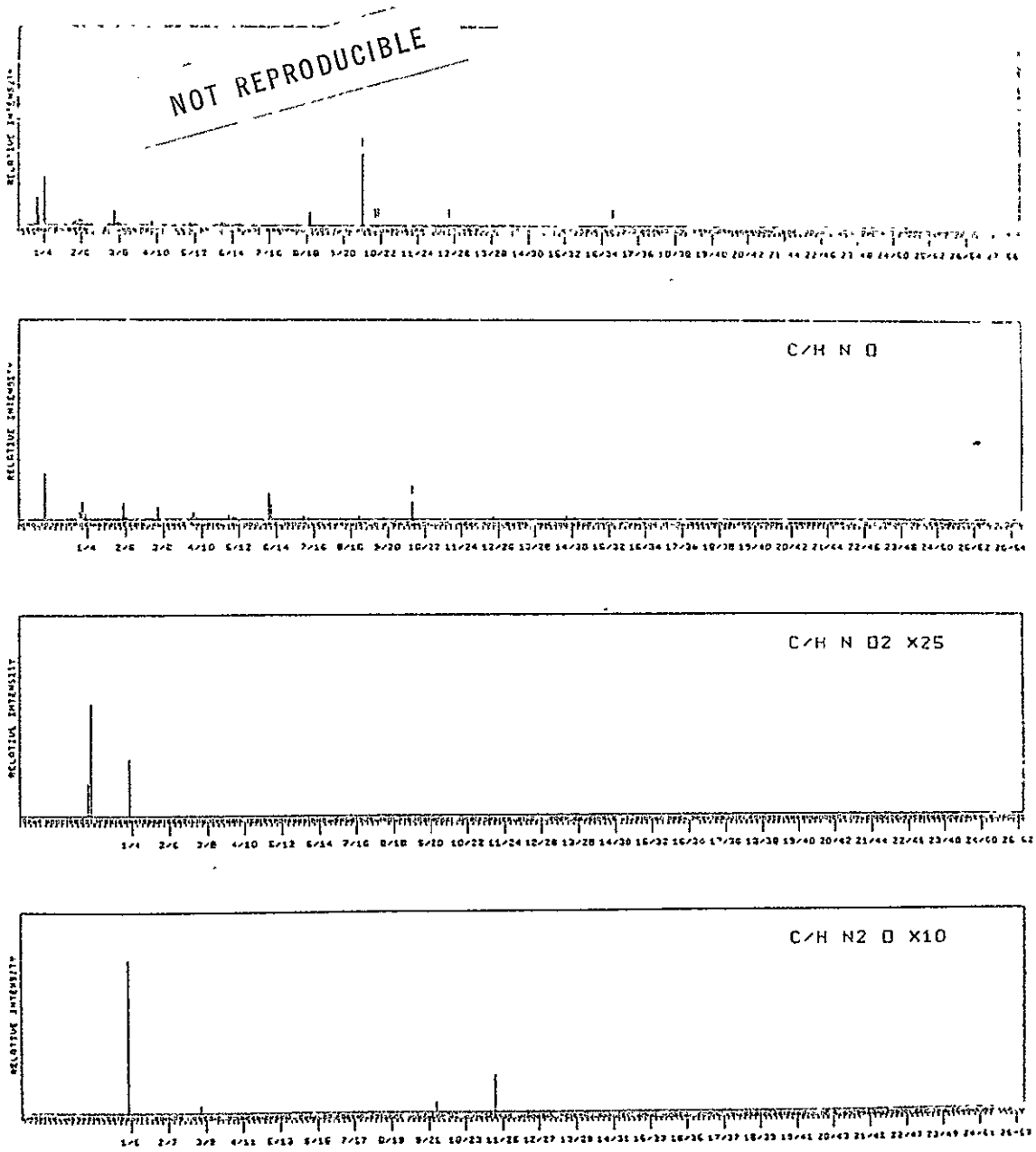

FIGURE 17-b. The partial high resolution mass spectrum of the Trap C extract from the model engine firing.

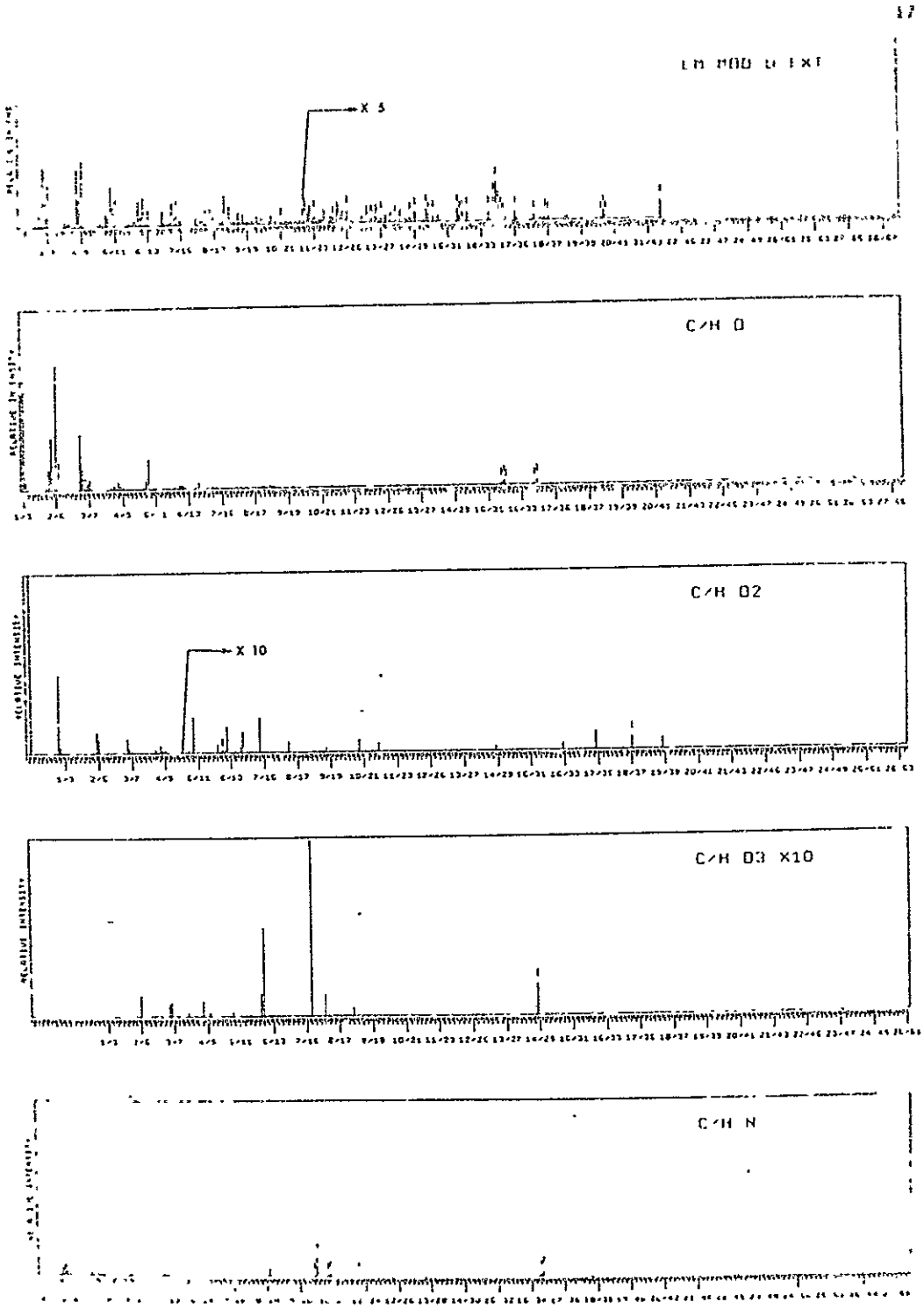

Figure 18-a. The partial high resolution mass spectrum of the Trap 0 extract from the model engine firing.

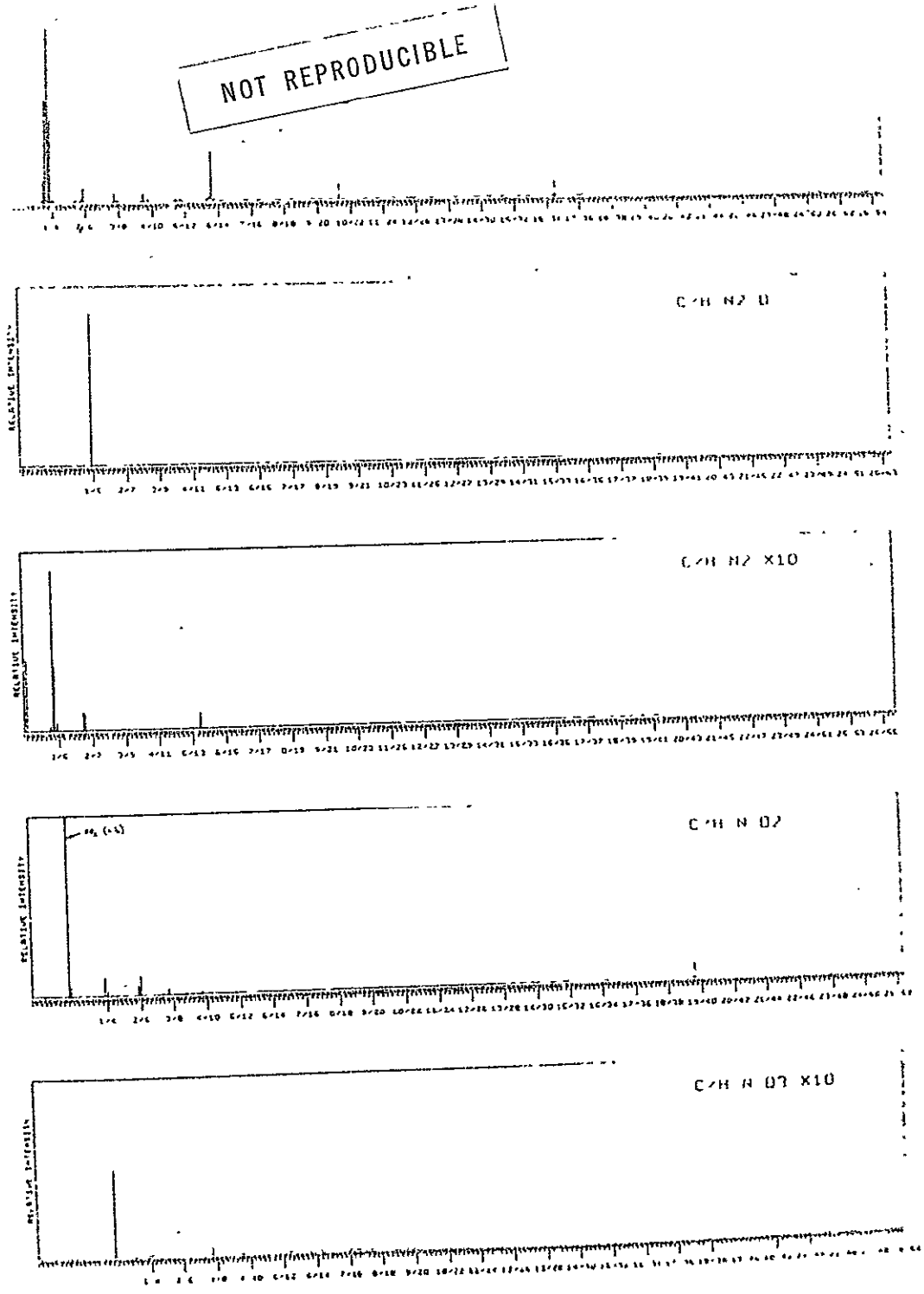

FIGURE 18-b. The partial high resolution mass spectrum of the Trap 0 extract from the model engine firing.

cannot be taken as quantitative measures, since the samples are benzene-methanol extracts and the more volatile components would have been depleted preferentially. Furthermore, ion intensities of molecules and fragments of varying heteroatom content, as well as differing structure, cannot be quantitated arbitrarily. The following molecules found (cf. Table III) are of specific geochemical interest due to their high inherent reactivity and/or tendency to form polymers: acetylene, HCN, CO, ethylene, formaldehyde, ketene, HCNO, dimethylamine, acetaldehyde, $CH_3-N=NH$, CH_3NO, NO_2, formic acid, HNO_2, acetone, nitromethane, and acetic acid. Other oxidation products of interest are briefly discussed. A series of C_4 hydrocarbons occur from m/e 50 to 57, C_4H_2 to C_4H_9 (C/H plot of Figs. 16 – 19), some which can be thought of as dimers of acetylene (structure VI) and ethylene (structure VII).

VI

VII

They can, of course, also arise from dehydrogenation reactions of the background hydrocarbons in the mass spectrometer, but the m/e 50 – 56 peak are significantly higher in the firing spectra (C/H plots of Figs. 17a, 18a, and 19a) than in the background (C/H plot of Fig. 16). The peaks at m/e 55, C_3H_3O (C/H O plot of Figs. 17a, 18a, and 19a) and m/e 56, C_3H_6N (C/H N plot of Figs. 17 , 18a, and 19b) can be thought of as reaction products (structures VIII and IX respectively).

$CH_2 = CH - C \equiv O^{\cdot+}$

VIII

$CH_2 - \overset{+}{N}H_2 - C \equiv CH$

IX

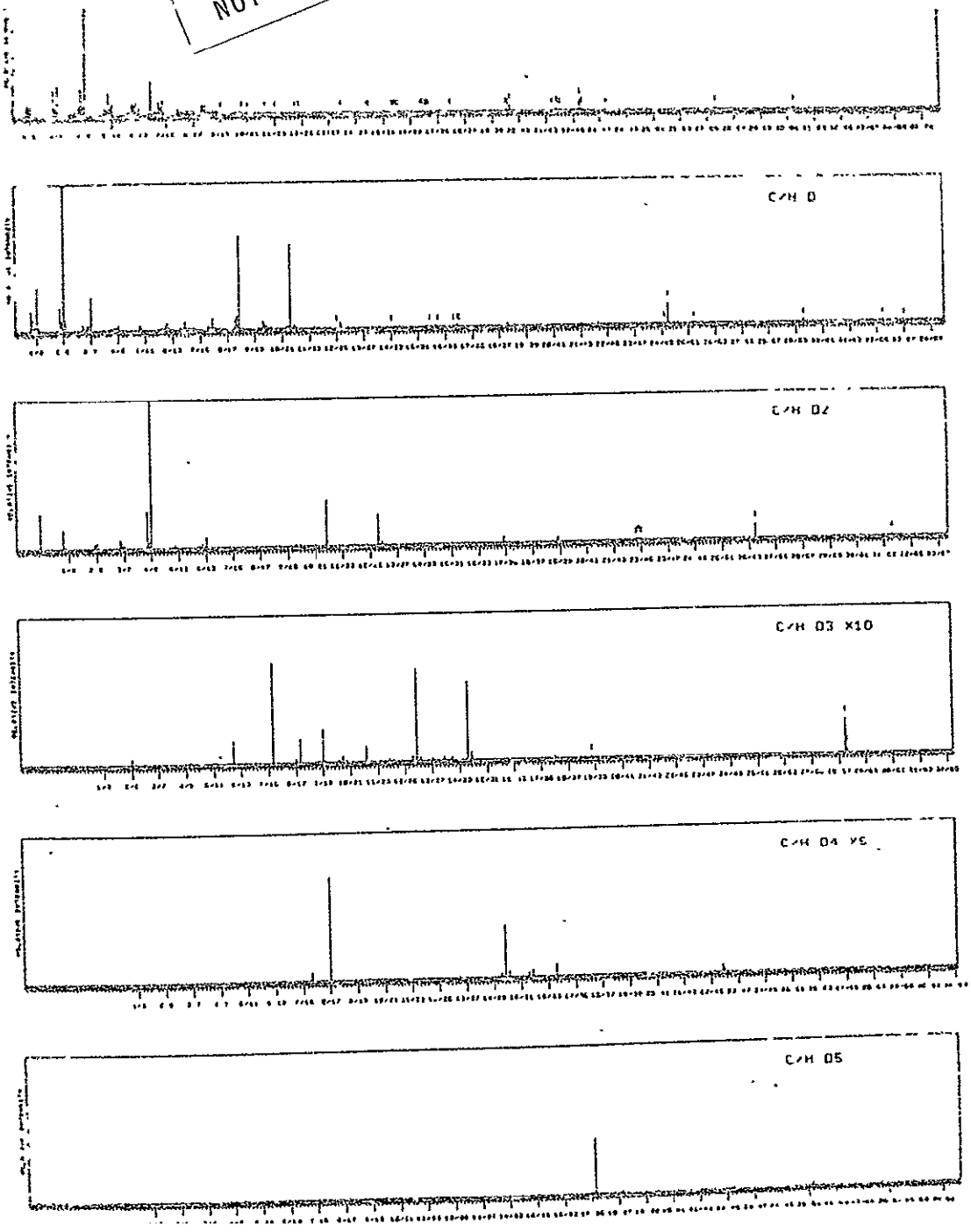

FIGURE 19-a. The partial high resolution mass spectrum of the Trap B extract from the Lunar Module Descent Engine firing.

FIGURE 19-6. The partial high resolution mass spectrum of the Trap B extract from the Lunar Module Descent Engine Firing.

The following higher mass peaks are derived by oxidative cleavage of UDMH: m/e 60, CH_4N_2O (C/H N_2O plot of Figs. 17b and 18b), structure X and (H NO (C H NO plot of Figs. 17b and 18b) nitromethane. The higher mass entries in Table III.

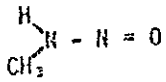

X

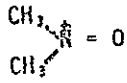

XI

are suspected to be reaction products of rocket exhaust with background and just background. To cite an example: ' Most hydrocarbon oils contain substantial amounts of olefinic hydrocarbons due to the cracking and refining processes. Nitric oxides (NO_2 N_2O_4) are strong oxidizing agents and the addition of NO_2 to olefins has been thoroughly studied:

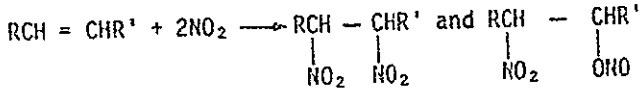

Such a reaction can account for the homologous series, $C_nH_{2n}NO$, ranging from n = 3 — 17 (C/H NO plot of Figs. 17 — 19) since γ-hydrogen transfer to eliminate an OH• radical is significant mass spectrometric fragmentation of nitroalkanes:

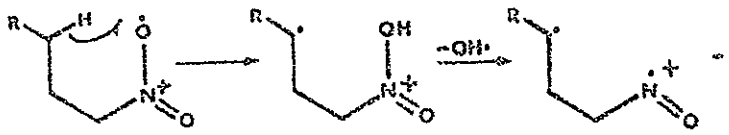

The dinitroalkanes and the nitro-nitrosoalkanes would not be expected to exhibit molecular ions but rather simple cleavage products as, e.g., structure XII, which then would undergo the γ-hydrogen transfer.

$$R - CH_2 - NO_2$$

XII

The high resolution mass spectral results of the LM Engine trap extracts were essentially the same as the already discussed LM 6-1 trap extract spectra. The trap B extract serves as illustration for these data in Fig. 19a and b and also to indicate a polymeric artifact found only in this extract. The low mass combustion products found in the Model extracts are also present in the Engine extracts (cf. Table III). The hydrocarbon and "octoil" background, as well as the "oxidized" background, are virtually the same as previously discussed. The major peaks in the high resolution data of trap B turned out to be homologous fragments of a polymer. The fragments due to direct cleavage (structure XIII) are m/e 91, C_7H_7:

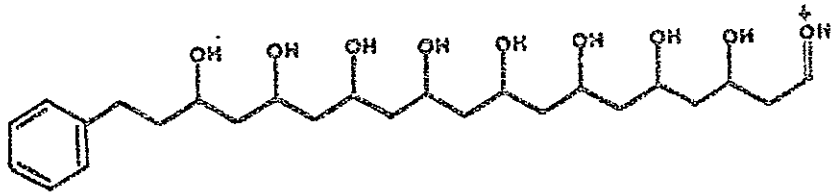

XIII

m/e 135, $C_9H_{11}O$; m/e 179, $C_{11}H_{15}O_2$; — detectable in increments of 44 mass units (composition C_2H_4O) to m/e 531, $C_{27}H_{47}O_{10}$. There is also a series

of peaks where the aforementioned fragments have lost an ether, alcohol or water. Referring to Fig. 19; $C_{21}H_{33}O_8$ (m/e 443) can be seen in the C/H O_8 plot, $C_{21}H_{33}O_7$ (m/e 399) in the C/H O_7 plot, etc., down to C_7H_7 in the C/H plot. The neutral fragment eliminated is C_2H_4O and the lowest member of the series is C_7H_7, thus the structure deduced was XIII, a polyvinylalcohol with a styrene end. Such polymers are used in paints, gels, etc..

As another indication of the complexity of these extracts the GLC patterns were run. A 1/8" x 5' column, packed with 3% SE-30 on chromosorb was used and usually programmed from 50-250° C at 6-8°/min and a helium flow rate of 30-40 ml/min.. Two examples of the trap background are shown in *Figure 20* (trap A) and *Figure 21* (trap B). The GLC trace for the model trap A extract is shown in *Figure 22*. The LM Engine trap B extract is shown by the GLC trace in *Figure 23*. No specific peaks were identified on any of the GLC traces run.

Recommendations and Further Background Samples

Due to the substantial weight of background organics, it was decided to check the whole system for contamination sources and attempt to reduce that background. On January 16, 1969, essentially the following recommendations were made at NASA White Sands Test Facility:

I. Solvents. 3:1 benzene-methanol (nanograde commercial rather than distill on site)

II. Glass Wool. Anneal glass wool after Soxhlet washing (extraction) in a muffle furnace at 350° C for minimum of three hours. Store it in chromic acid cleaned glass containers.

III. System Cleaning and Assembly
   - A. Rewold (butt weld) trap bottoms
   - B. Buff scaly welds
   - C. Omit Freon cleaning
   - D. Final cleaning step should be with 3:1 benzene-methanol instead, as follows: detergent bath, tap water, distilled water, 3X methanol, 2Y with 3:1 benzene-methanol, put in glass wool, seal and bake out.

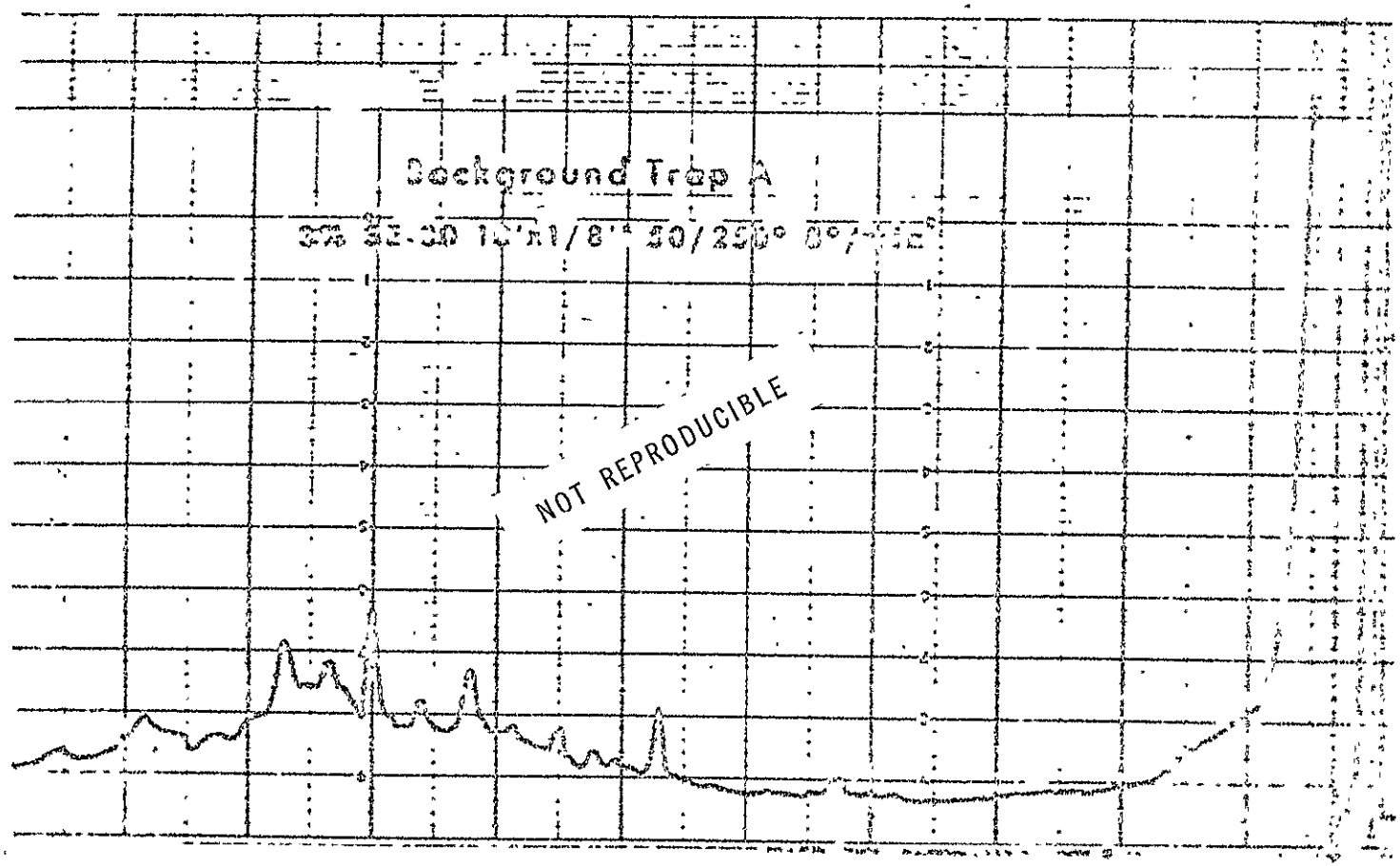

FIGURE 22. The gas-liquid chromatogram of the background extract from Trap A.

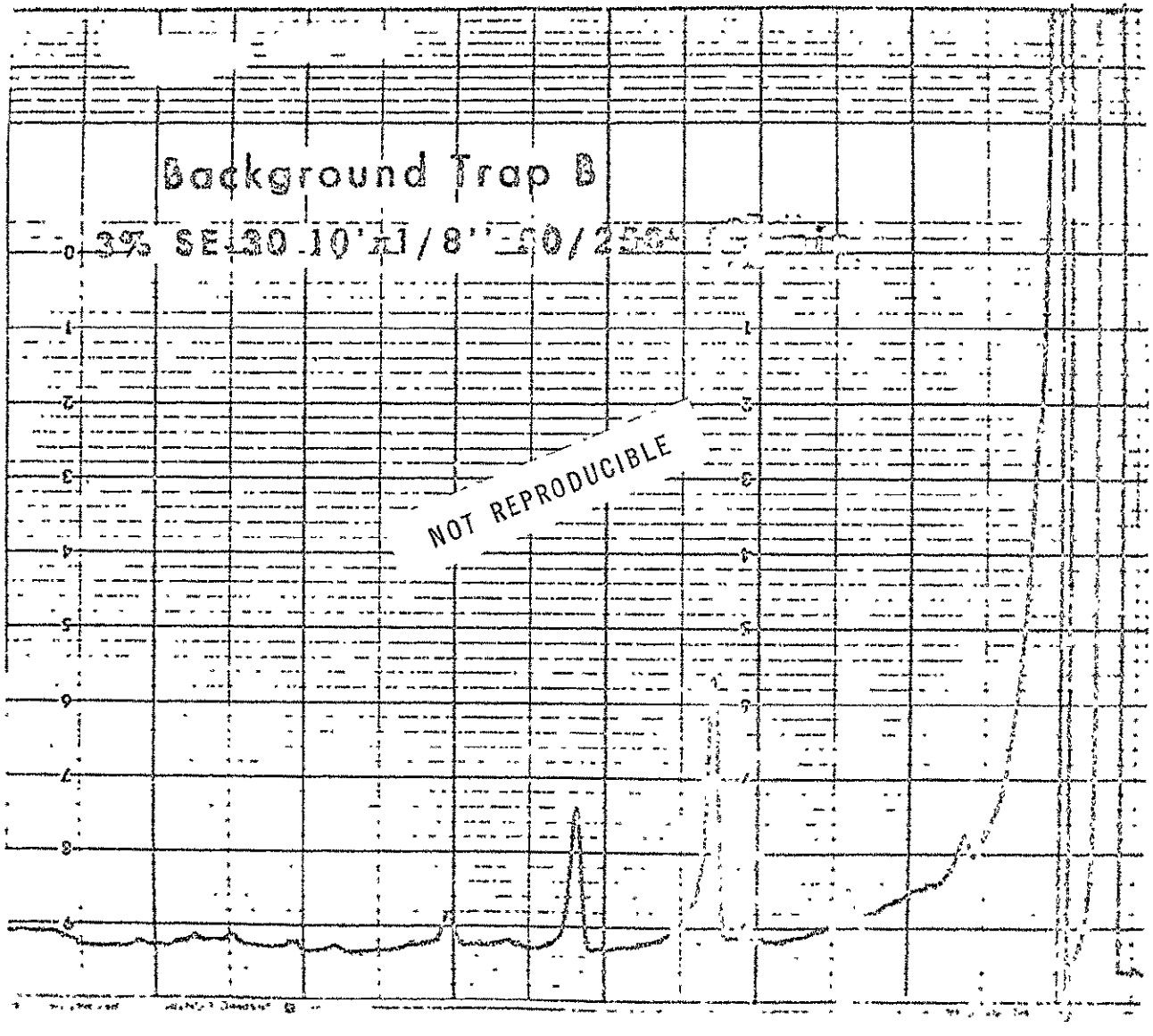
Background Trap B
NOT REPRODUCIBLE

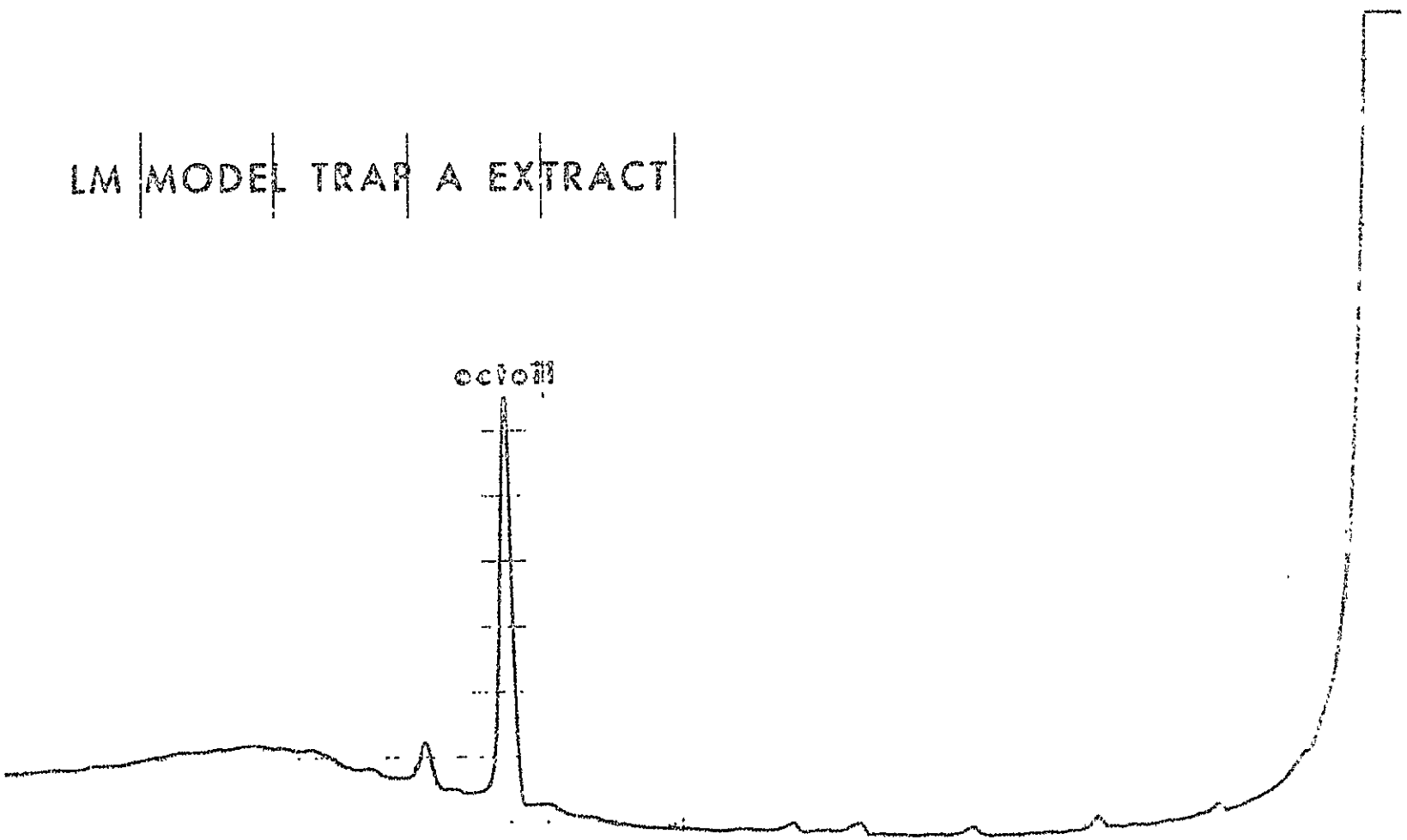

FIGURE 22. The gas-liquid chromatogram of the extract from Trap A, LM [illegible] Engine [illegible].

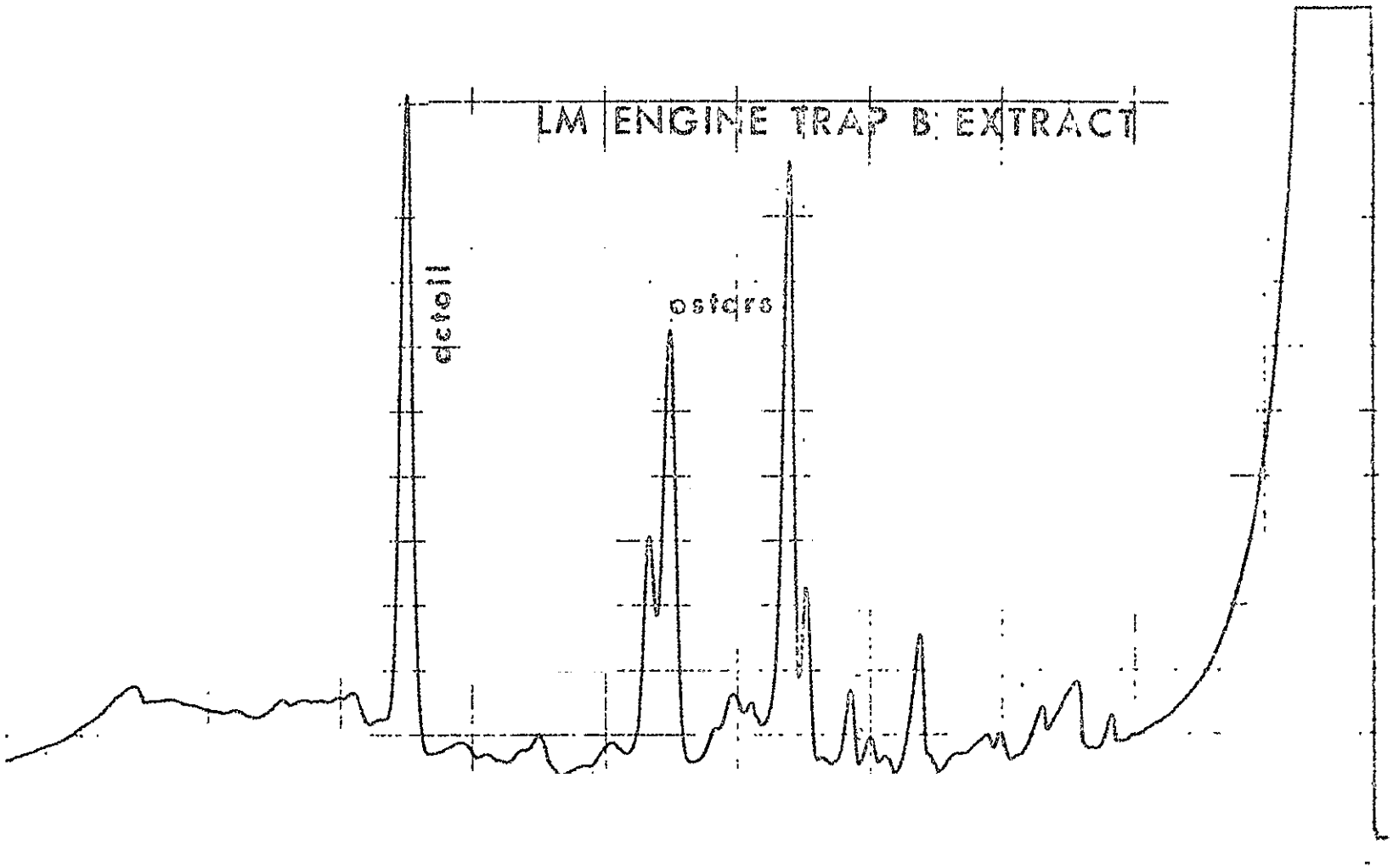

FIGURE 23. The gas-liquid chromatogram of the extract from Trap B, LM Descent Engine firing.

E. Valve flanges with knicked knife edges should be replaced

Further samples were taken at that time to evaluate their background contribution. Trap C (it had been through the cleaning process and bakeout) was taken off a fully prepared sampling system and extracted with 3:1 benzene-methanol by the identical procedure applied to the previous traps analyzed. The extract weighted 10.6 mg residue and had the same appearance as the other background extracts. A sample of solvent cleaned glass wool packed in polyethylene was also extracted with 3:1 benzene-methanol, using ultrasonication. Approximately 50% of the solvent mixture added was recovered by draining off, the remainder being held up by the glass wool, and this extract was filtered through a fine frit filter to remove small glass wool fibers. The solvent was removed under vacuum yielding a residue of 17.4 mg having the same appearance as the background extracts. The polyethylene bag (15" × 10") used to store the glass wool was extracted separately with 3:1 benzene-methanol and the extract yield was 10.3 mg of colorless oil after solvent evaporation. Four Viton O rings (2 per Varian Value, 2 valves per trap) were allowed to soak in 3:1 benzene-methanol overnight, yielding 3.4 mg of a dark yellow oil upon solvent removal.

The GLC of the polyethylene bag extract shown in *Figure 24* and the low resolution mass spectrum in *Figure 25*. The main constituents of this extract are octoils (various phthalic acid esters) and hydrocarbons. The ions at m/e 167 and 149 represent structures XIV and XV, respectively. The hydrocarbons are established present by the peaks grouped around C_nH_{2n+1} ranging from n = 2 – 30$^+$.

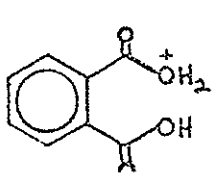

XIV

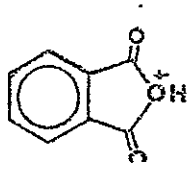

XV

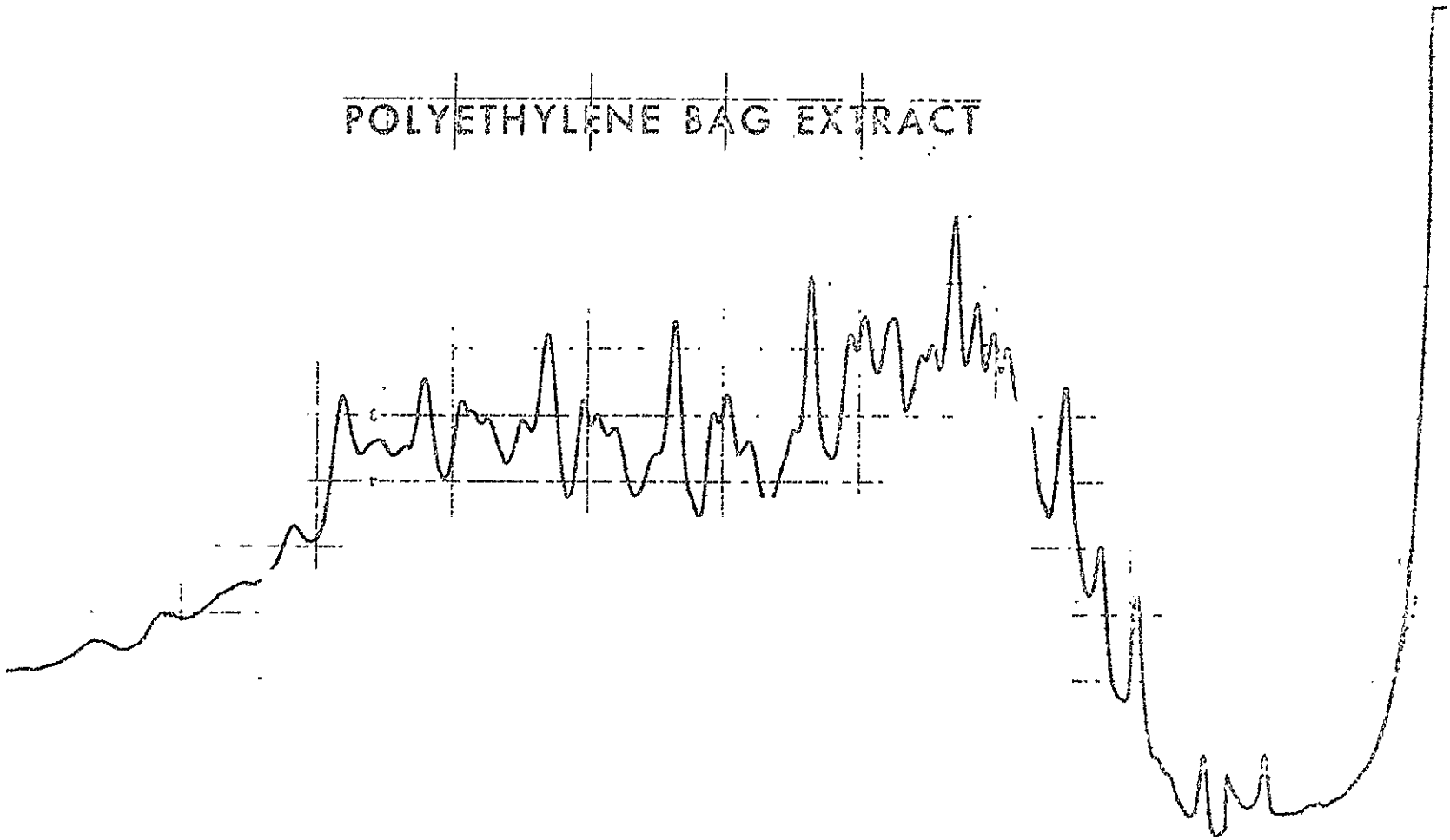

FIGURE 24. The gas-liquid chromatogram of the benzene/methanol extract of a polyethylene bag.

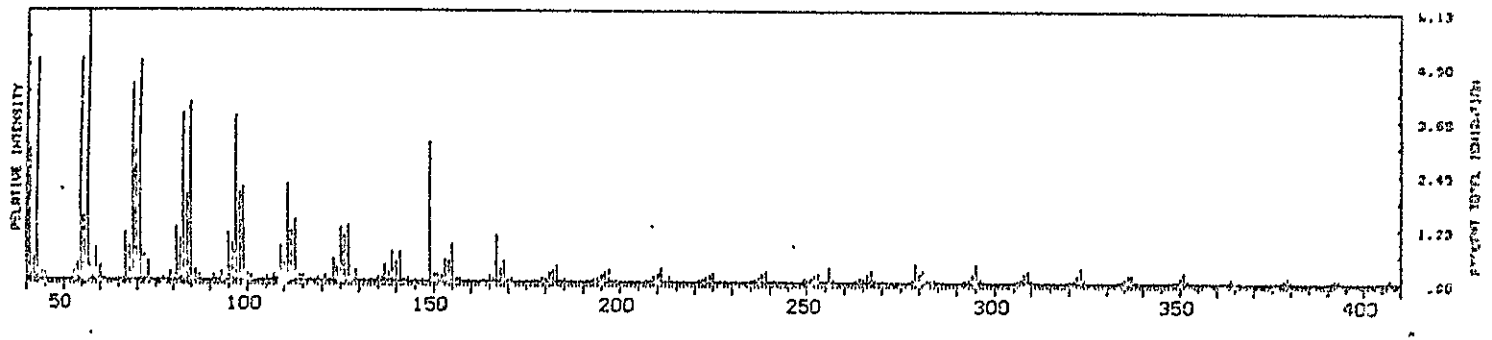

FIGURE 25. The low resolution mass spectrum of the polyethylene bag extract.

The Viton O ring extract was also chromatographed and the trace is shown in *Figure 26*. Several low resolution mass spectra were taken, two of which are shown in *Figures 27a* and *27b*. The major component of the *a* spectrum appears to have a composition $C_{22}H_{12}$, structure XVI, as well as a general assemblage of fluorohydrocarbons (base peak m/e 69, doublets m/e 85, 101, etc.).

Coronene 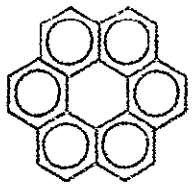

XVI

The major constituents of the *b* spectrum appear to be a nitrogen containing C_{29} aromatic at m/e 383 and a $C_{22}H_{36}$ aromatic and $C_{24}H_{12}$ aromatic doublet at m/e 300. The fluorohydrocarbons appear also in this spectrum as a general background.

The recommended new cleaning procedures of January 16, 1969 resulted in a substantial decrease in background. The glass wool which was solvent extracted and then baked at 350° C for three hours had an organic extract residue of 0.9 mg as compared 17.4 mg for unbaked glass wool. The extract weights of the traps from firing Series V, Test 003 are also significantly lower (cf. Table II). It should be noted that trap D of this set was lost — the glass wool had blown into the valve seat. The gas chromatograms of the trap extracts had the preliminary appearance of hydrocarbon oil and "octoil". High resolution mass spectral studies on this extract set as well as Series V, Test 004 extracts are in progress. A sample of turbine pump oil and the residue from A-50 fuel are also under investigation.

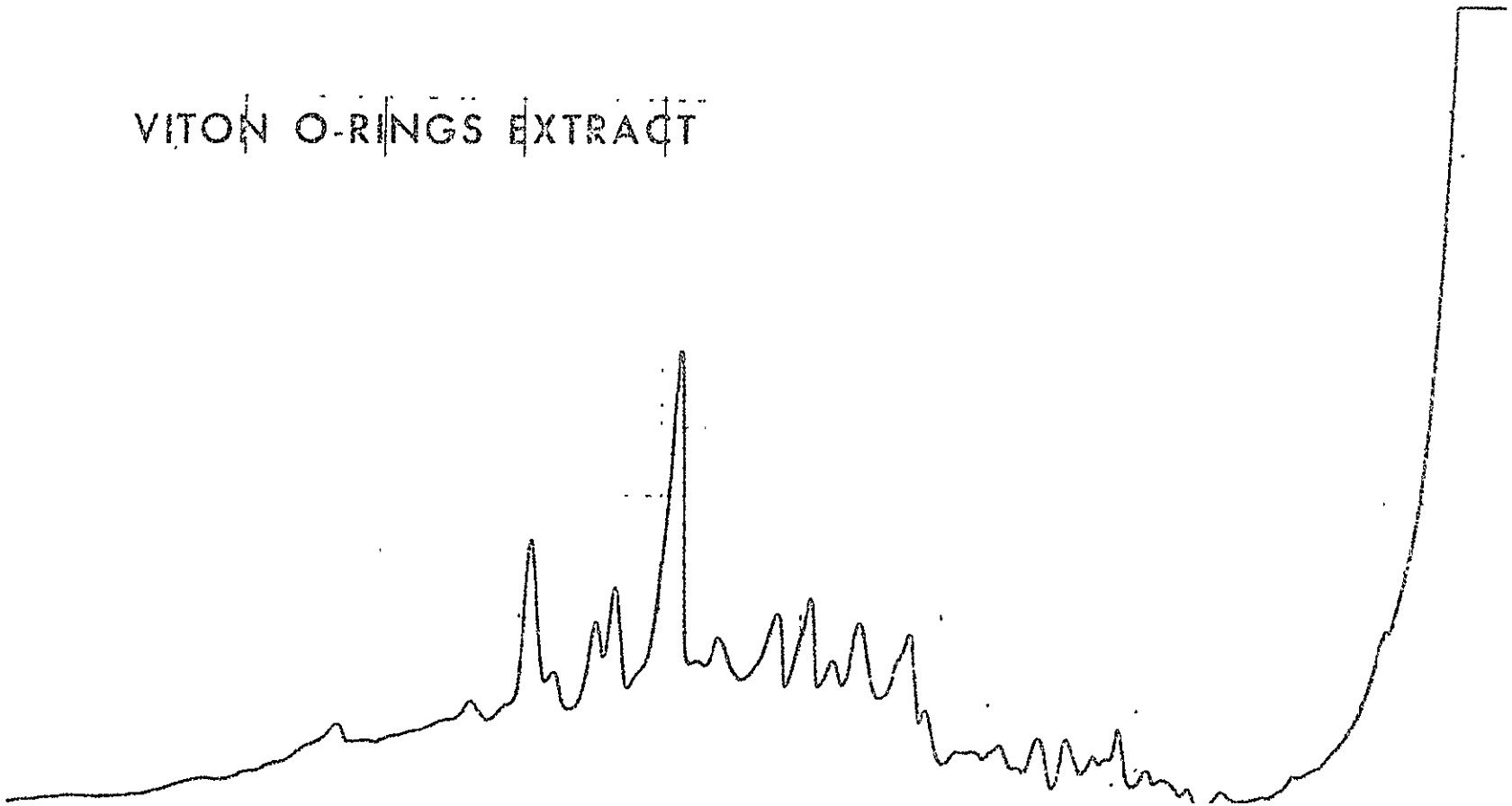

FIGURE 26. The gas-liquid chromatogram of the benzen/methanol extract of four Viton O rings.

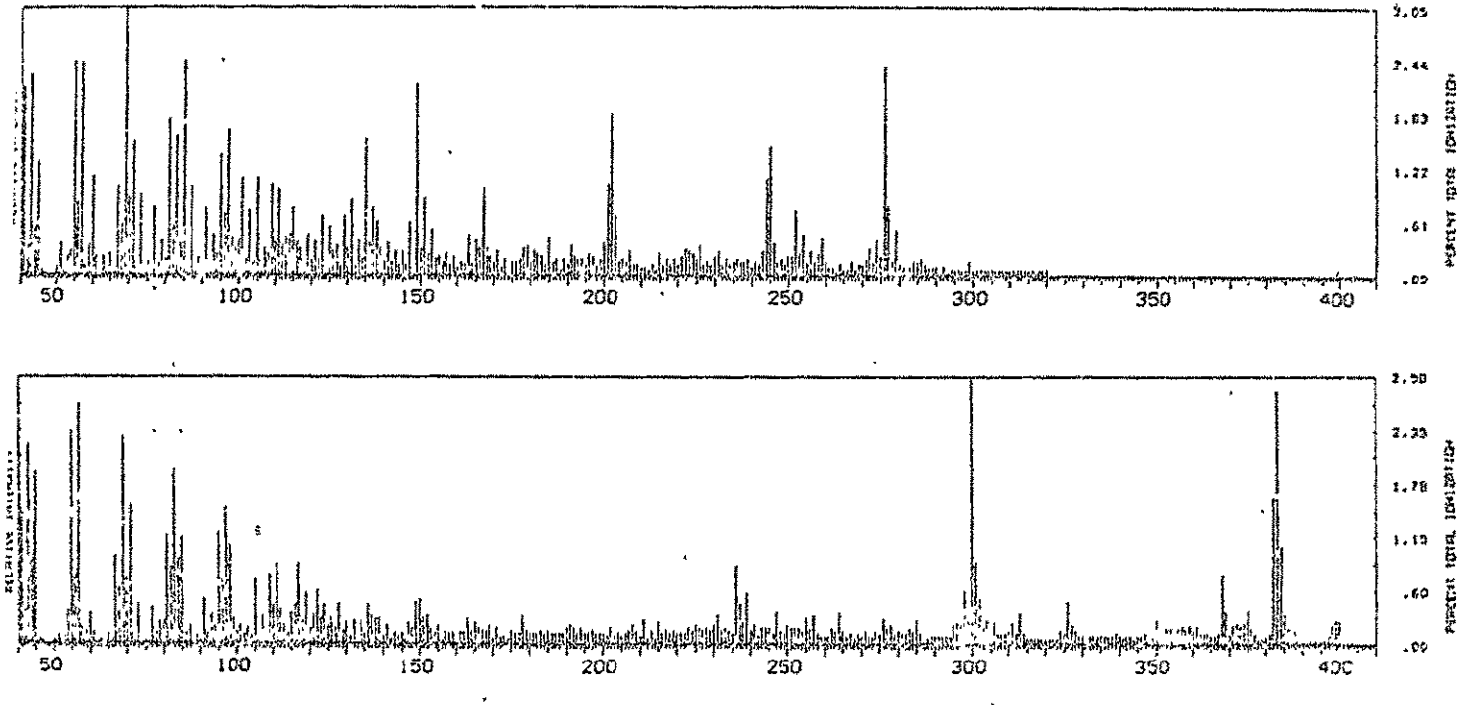

FIGURES 27-a and b. Two low resolution mass spectra of the Viton O ring extract.

V. FACILITIES IMPROVEMENT

Construction of an Isotope Ratio Mass Spectrometer for Stable Isotope Geochemistry

The measurement of the relative abundance of the stable isotopes of carbon has proven to be a powerful technique in organic geochemistry. Examples of its use in studying Precambrian photosynthesis, detecting contaminated samples and learning about diagenesis of organic matter in sedimentary rocks are reported in the literature. The emphasis in this laboratory on the use of mass spectrometric techniques for the analysis of returned lunar material makes it logical that this tool be available.

A mass spectrometer for the measurement of small variations in C^{13}/C^{12} ratios in samples of geochemical interest is under construction. The instrument is a single focusing, 90° sector instrument with a radius of curvature of 12". The ion source is a modified Consolidated Electrodynamics Corporation Type D 143680. A double collection system based on the design of Nier has been constructed and installed. The ion source and analyzer are pumped differentially. The source region has an ion pump of 130 liters per second capacity. The analyzer and collector are pumped by an oil diffusion pump with a liquid nitrogen trap. The pumping speed will be about 100 liters per second. The main vacuum system, mass spectrometer tube, ion source and collector have been completed and the system is vacuum tight. The assembly is now being pumped and baked out. A base pressure of about 10^{-8} torr is expected.

All of the major electronic units have been installed and given a preliminary testing. A few small control units are under construction. A gas switching mechanism and dual inlet system based on McKinney's design is under construction. All parts have been fabricated and assembly will start in a few weeks. An innovation of the inlet system is the use of stainless steel bellows instead of a mecury ram for adjustment of sample pressures. This should result in a much cleaner vacuum system and permit the use of smaller samples.

It is estimated that preliminary measurements of isotope ratios on tank carbon dioxide will start in 4 to 6 weeks.

A sample combustion system, carbonate generating line and carbon dioxide purification apparatus will be constructed in the room with the mass spectrometer. All of the necessary parts have been ordered and will arrive the next four weeks. The system is based on a design that has been in steady use for the past 10 years. Its setup and operation should present no unusual problems.

During the next six months, a complete stable carbon isotope laboratory should be placed into operation. The first experiments to be done after the mass spectrometer and preparation lines are operative is to setup some laboratory working standards. These materials will be compared closely with National Bureau of Standards Isotope Reference Samples 20, 21, and 22.

When the working standards have been satisfactorily calibrated, the initial geochemical experiments will be started. A comparison of the C^{13}/C^{12} ratios in selected fractions of the Green River Shale will be made. During the calibration and initial experiments, chemists permanetly employed at the laboratory will be instructed in the mass spectrometric and preparative techniques.

Perkin-Elmer 270 Mass Spectrometer

A Perkin-Elmer 270 combination gas chromatograph — mass spectrometer was purchased during this period for use in routine analysis of organic geochemical mixtures and to provide low resolution mass spectra for mechanistic mass spectrometry studies. The hookup of the gas chromatograph to the mass spectrometer precludes collection of individual components of mixtures on a separate gas chromatograph, a time consuming and often inefficient process. Rapid identification of the components of complex mixtures is now possible. The instrument has been connected to a Sigma 2 computer to facilitate the acquisition and processing of the enormous amount of data routinely obtained.

The instrument is now being checked for sensitivity, efficiency of the vacuum system, and optimization of operating conditions. The aim is to be able to obtain high quality mass spectra from submicrogram quantities of individual compounds and mixtures.

Over the next six months this testing will continue and several modifications will probably be made. A heated glass inlet system will be added for increased flexibility in sample introduction. The present inlet systems are the gas chromatograph and a direct introduction probe which inserts a sample directly into the ionization chamber. The design of the direct introduction vacuum system may be changed since the present one is inconvenient and inefficient. Several electronic modifications are also planned.

Cleanroom Preparation

The next six months will see a concentrated preparation for analysis of returned lunar samples. Part of the cleanroom currently being used by the Mariner Mars Group at the Space Sciences Laboratory will be converted for this purpose. The goal is to obtain a room as "organic — free" as possible. After the room is cleaned, attempts will be made to determine the level and source(s) of possible contamination. Test analyses on a low-level organic sample (e.g., the recently acquired meteorite, rosequartz, or a Precambrian sample) will also be performed. Chemicals and solvents must be carefully checked for contamination and purified as necessary. New glassware will be purchased as well as an annealing oven to maintain the glassware free of interfering organic substances.

PERSONNEL

Dr. A. L. Burlingame	Principal Investigator
Dr. Thomas C. Hoering	Visiting Research Chemist
Dr. Peter Schulze	Assistant Research Chemist
Dr. Dennis H. Smith	Assistant Research Chemist
Dr. Joachim G. Liehr	Post-Graduate Research Chemist — IV
Dr. Troy Story	Post-Graduate Research Chemist — V
Richard W. Olsen	Senior Development Engineer
Fred C. Walls	Specialist
Bernd R. Simoneit	Spectroscopist
James T. Wilder	Spectroscopist
Robert E. Furey	Junior Development Engineer
Paul Harsanyi	Junior Development Engineer
Joan M. Tesarek	Research Assistant
Jan S. Hauser	Senior Electronics Technician
Michael T. Issel	Senior Electronics Technician
Deborah Allen	Programmer
Kenneth Jacker	Assistant Programmer
Galen M. Collins	Electronics Technician

Sydell Gelber	Lab Technician
Ellen Scott	Lab Technician
Claude Sprowls	Lab Technician
Gene H. Tobias	Lab Assistant
Nancy L. Twombly	Secretary

PUBLICATIONS

Schulze, P. and A. L. Burlingame, Formation and Detection of Metastable Ions in a Double-Focusing Mass Spectrometer, *J. of Chemical Physics*, 4870 (1968).

Schulze, P., B. R. Simoneit, and A. L. Burlingame, A Combined Electron Impact-Field Ion Source and its Applications to Organic Geochemistry, *J. Mass Spectrometry and Ion Physics*, *2*, 183 (1969).

Richter, W. J., B. R. Simoneit, D. H. Smith, and A. L. Burlingame, Detection and Identification of Ketocarboxylic and Dicarboxylic Acids in Complex Mixtures by Reductive Silylation, and Computer — Aided Analysis of High Resolution Mass Spectral Data, *Anal. Chem.*, submitted.

Han, J., B. R. Simoneit, A. L. Burlingame, and M. Calvin, Organic Analysis on the Pueblito de Allende Meteorite, *Nature*, in press.

Burlingame, A. L., and B. R. Simoneit, High Resolution Mass Spectrometic Studies of Green River Kerogen Oxidations, *Nature*, in press.

Tesarek, J. M., Mass Spectral Fragmentation of Selected Saturated Heterocyclic Molecules, Ph.D. Dissertation, U. of California, Berkeley, 1969.

Burlingame, A. L., D. H. Smith, R. W. Olsen, and T. O. Merren, Real Time High Resolution Mass Spectrometry, *Computers in Analytical Chemistry* (Vol. 4 in Progress in Analytical Chemistry series) C. H. Orr and J. Norris, Eds., Plenum Press, New York, September, 1969.

TALKS

Burlingame, A. L., Real-Time High Resolution Organic Mass Spectrometry, Eastern Analytical Symposium, New York City, November 13, 1968.

Smith, D.H., Real-Time High Resolution Mass Spectromery, Pacific Conference on Chemistry and Spectroscopy, San Francisco, November 6, 1968.

Hoering, T. C., Optically Active Alkanes in a Petroleum, Meeting of the Group for the Analyses of Carbon Compounds in Carbanaceous Chondrites and the Returned Lunar Sample, Tempe, Arizona, December 5 — 6, 1968.

Hoering, T. C., Organic Geochemistry and the Record of Ancient Life, Symposium on the Origins of Life, California State College at Los Angeles, February 13, 1969.